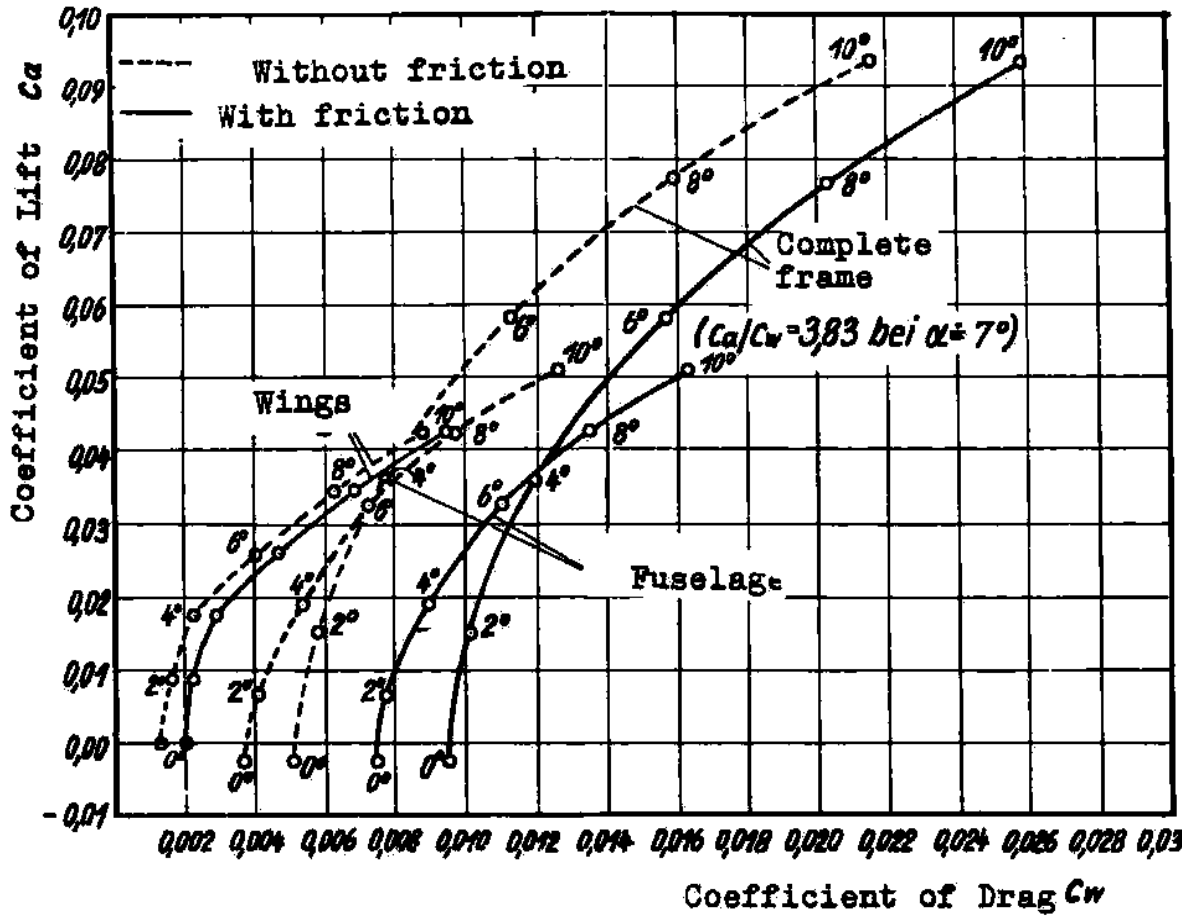

Figure 36; Computed polars of the wing, the fuselage, and of the entire frame of the Rocket Bomber at M = 3. (The aerodynamic coefficients are based on the area of the lifting surfaces.)

excitation of molecular vibrations are reached, then considerable oscillation can occur in the available streaming time, i.e., $\varkappa$ approaches 1.29. For $\varkappa = 1.4$ the pressure on a flat surface is $p/q \doteq 2.4 \sin^2\alpha$. The corresponding pressure in the case of a cone with stream along its axis is, according to Busemann and Guderley, $p/q \doteq 2.1 \sin^2\alpha$. If the wall surface is curved in the direction of the streaming, the layer streaming off along the wall must follow this curvature and undergoes acceleration perpendicular to the plate, so that for convex curvature a negative additional pressure p_2 results. For $\varkappa = 1$, these were calculated by Busemann for general curvatures. For the important case of constant radius of curvature the equations can be integrated and give for the lens profile $-p_2/q = \sin^2\alpha_s - \sin^2\alpha$ and for the ogive-shape, $-p_2/q = \frac{1}{3}\sin^2\alpha_s + \frac{1}{3}(1-\cos\alpha_s\cos\alpha) - \frac{1}{3}\sin^2\alpha$ where α_s is the angle of attack for the first surface element. Thus the air pressure drops very rapidly as we move back from the end of the object, and vanishes, in the case of the lens profile, at the point for which the angle of attack is $\alpha_s/\sqrt{3}$; for the bullet shape it vanishes somewhat later, at $\alpha/\sqrt{8}$, so that the average pressure on the curved surfaces is far less than for plane surfaces. For $\varkappa > 1$ the centrifugal effects, according to Busemann and Guderley, are somewhat larger, so that the pressures for $\varkappa = 1.4$ are 7% smaller than for $\varkappa = 1$, in the case of the lens profile.

As regards the frictional stresses parallel to the wall between the fixed surface and the air, for dense air, momentum parallel to the wall is transferred to the wall only by a thin boundary-layer of molecules near the wall, so that the usual friction laws are valid. One is led, in the case of high supersonic velocities, to give main importance to laminar frictional effects, so that the friction is determined by V. Karmans formula $\tau/q = 1.3/\sqrt{Re}$. In the valleys of the flight path of the aircraft, which determine the energy consumption, we may use a value of $Re = 10^8$, which gives $\tau/q = 0.00013$ for flat, untilted surfaces. At finite angles of attack, the density, friction and temperature change on the leeward side (negative angle of attack) become zero, while for the windward side they are 6 times as great as for free air; at the same time the viscosity of the air increases with the stagnation temperature $V^2\sin^2\alpha/2000$ according to the relation

$$\eta = 1.753\times10^{-6}\left[(273 + V^2\sin^2\alpha/2000)/273\right]^{0.76}$$

The frictional forces on the surfaces to windward are approximately

$$\tau/q = 6\times1.3/\sqrt{6\,Re\left[(273 + V^2\sin^2\alpha/2000)/273\right]^{0.76}}$$

With the aid of these equations we can calculate the aerodynamic forces on an arbitrary body for $V/a \to \infty$. Fig. 37 shows the polars first for the infinitely thin flat plate which is known to be theoretically the best wing for flight above the velocity of sound, second for the wedge profile with flat sides and a thickness 1/2 of the wing depth in the second third of the profile (8, p. 170) and finally for the symmetric double-convex lens profile composed of two equal circular arcs, also with thickness 1/20 of the depth. In the region of $V/a = 1$ to 3, where the linear dependence of the aerodynamic forces on the angle of attack is valid, and where the excess pressures on the windward surfaces and the subnormal pressures on the leeward surfaces are of the same order of magnitude, the biconvex lens profile gives the best glide-numbers; in the Newtonian region, where the air pressure varies quadratically with the angle of attack, and where the air pressure vanishes in the shadow region, the flat-surfaced wedge profile is definitely superior. In the region of angles of attack which are greater than the front bevel angle of the wedge, it is as good as the infinitely thin flat plate. In addition it has the remarkable property, in this velocity range, that the ordinarily strict requirement of minimum profile thickness is weakened, in the sense that even the limiting profile can be so thick that the whole wing surface is in the shadow. The inferiority of the lens profile to the wedge profile in this velocity region arises from the fact that larger angles of attack give poorer glide-numbers; since the pressure depends quadratically on the angle of attack, the large angles for the front parts of the surface outweigh the effect of the small angles at the back parts so that altogether a poorer glide-number results than for the flat underside of the wedge profile. A further reason for the inferiority of the lens profile is that the curved surface, because of the centrifugal action, is acted upon by smaller normal pressures and about the same frictional stresses as for the wedge profile; thus to obtain the same lift, larger surfaces must be used, which involves not only greater weights but also greater frictional forces. Since the rocket bomber needs the best possible glide number at high velocities, it should be designed with wings having a wedge profile.

These considerations can in principle be extended to spatial flow. Fig. 38 shows the polars for 3-dimensional flow around three surfaces with equal projected area and the same height which might be considered for the bow shape - a circular cone with height four times the diameter of the base, a bullet with the same height and base diameter (16.25 caliber radius), and finally a half-bullet with the same height and a semicircular base of the same size as that of the two surfaces of revolution, i.e, with 8.25 caliber radius. The aerodynamic coefficients are all for

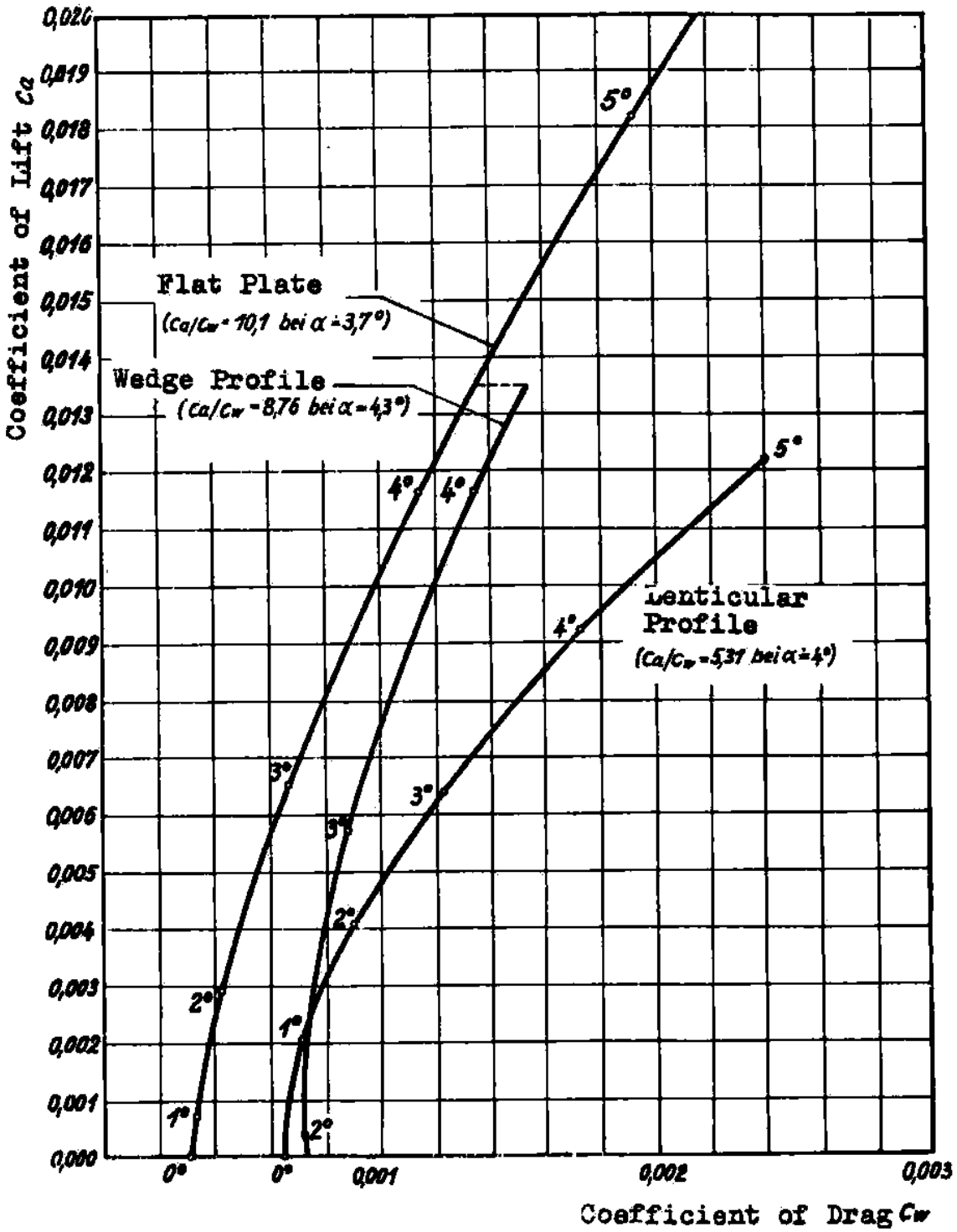

Figure 37; Polars of a plane curface, a wedge profile and a lenticular profile at M=3 (The aerodynamic coefficients are based on the area of the lifting surfaces)

the same projected area. While the cone and bullet differ little in glide-number, the half-bullet with flat surface to the front, is far superior, having a glide-number with $1/\varepsilon = 4.12$. This is of decisive importance for the shape of the fuselage of the rocket bomber. While in the region V/a = 1 to 3, the bullet has the optimum glide-number, the laws determining the shape of a body under 3-dimensional flow change for high Mach numbers in the same way as for the wing sections; on the under side of the surface, which mainly determines the magnitude and direction of the net aerodynamic force, the air pressure should be as large, and the resistance components as small, as possible. The underside should consist solely of surfaces tilted toward the course wind. For a given average angle of attack of the undersurface, and for quadratic dependence of pressure on angle of attack, one obtains the best ratio of drag to lift on the underside if it is curved as little as possible in the direction of flow. On the upper side of the body, which with proper shape is unimportant for determining the total aerodynamic force, the pressures should be as small as possible. Therefore, the upper side should preferably consist only of surfaces tilted to leeward. If this is not possible, the parts of the upper surface which are to windward should have the smallest possible angle of attack, and be curved convex to the direction of flow, to keep the streaming pressure low by taking advantage of the centrifugal effect of the airmass streaming off the curved surface. Summarizing, for large Mach numbers, bodies should be so streamlined with a point or dihedral at the front, that the lifting undersurface is not curved in the direction of streaming, and that the upper surface should consist as far as possible of surfaces to leeward; the unavoidable windward sections of the upper surface should have a convex curvature in the direction of flow. (29)

The fuselage of the rocket bomber was shaped in accordance with this recipe; its polars for $1/\varepsilon \to \infty$ are shown in Fig. 39. From the figure we see that the optimum angle of attack for wings and fuselage are $\alpha = 4°20'$ and $\alpha = 8°30'$ resp. Since the wing surface is smaller than the fuselage surface, the more favorable glide-number for the wings has little effect compared to that of the fuselage, and one finds a theoretically most favorable angle between wings and fuselage of -2° for which the optimum reciprocal glide number $1/\varepsilon = 6.51$ is obtained for angle of attack $\alpha = 5°30'$ for the wings and $\alpha = 7°30'$ for the fuselage. For constructional reasons, and also to have simple streaming conditions at the wing roots, the angle of incidence was chosen as 0°; the polar for this case is shown in Fig. 36, which shows a best $1/\varepsilon = 6.4$ for $\alpha = 7°$. This value of glide-number, which can be attained by proper shaping of the fuselage and wings, is surprisingly favorable for high supersonic speeds, and is scarcely different from that of present aircraft below the velocity of sound. We may safely assume, for the velocity range $\frac{V}{a} = 30$ to 10, that the results derived for $1/\varepsilon \to \infty$ still apply, and that below this range the characteristics for $\frac{V}{a} = 1$ to 3 gradually appear.

On the basis of the previous investigation the variation of glide number of the rocket bomber for various angles of attack can be represented as in Fig. 40 for the whole range of velocities in dense air. The very favorable glide-number below sound-velocity, $\varepsilon = \frac{1}{7.75}$ at $\alpha = 5°$, drops very rapidly as we approach the velocity of sound, then takes on the value $\varepsilon = \frac{1}{3.8}$ at $\alpha = 8°$ for velocities slightly above the velocity of sound. Above $\frac{V}{a} = 3$, the glide-number improves and then rapidly approaches its favorable behavior for high Mach numbers, with

$$\varepsilon = \frac{1}{6.4} \quad \text{at} \quad \alpha = 7°$$

In all the previous considerations on the aerodynamic forces, the air was considered as a continuous medium. As the later sections show, the path of the rocket bomber reaches heights of over 1000 km. There the density of the air becomes so very small that on the one hand the stagnation pressures for even extreme velocities no longer result in aerodynamic forces at all comparable with the other external forces on the aircraft, and also the laws for calculating the aerodynamic forces are no longer those derived for a continuous medium. Fig. 41 is a plot of the air density ρ as a function of the height H for values up to 20,000 m from the well known formula for a homogeneous isothermal atmosphere; for heights between 11 and 22 thousand m, the relation is $\rho/\rho_0 = 1.6839\, e^{-H/6341}$ (see also "Dinorm 5450" or (33)). This expression for density at great heights is used in the later (note: original has error; uses ρ instead of $\rho(T,H)$) calculations. It is frequently assumed that the composition of the atmosphere at high altitudes is the same as on the ground - i.e., mostly N_2 and H_2, but that these materials are more or less dissociated into atoms. Therefore two dotted curves in Fig. 41 are used to show the density if all molecules are dissociated into atoms (left curve), and if only a partial dissociation occurred, as assumed by Godfrey (middle curve). The molecular free path for constant composition varies with the density according to the relation $\lambda[cm] \doteq 10^{-7}\, \rho_0/\rho$. This relation also holds approximately for the dotted curves for the dissociated atmosphere, since the effect of dissociation on the free path is of the same order as the error in determination of the free path. At heights of 40 km, the free path is already greater than the thickness of the laminar boundary layers (10^{-4}–10^{-5} m), reaches the size of the aircraft dimensions at a height of 120 km., and rises to over 1000 km. at a height of 200 km. The stagnation pressure corresponding to the "velocity of escape" V = 12000 m/sec is less than 1 kg/m2 at 100 km. altitude; i.e., at 100 km. altitude the aerodynamic forces have practically disappeared, and the motion of the rocket bomber is along practically a pure inertial path. The expressions derived for the aerodynamic forces on the assumption of a continuous medium are already invalid at heights over 40 km, since the distances

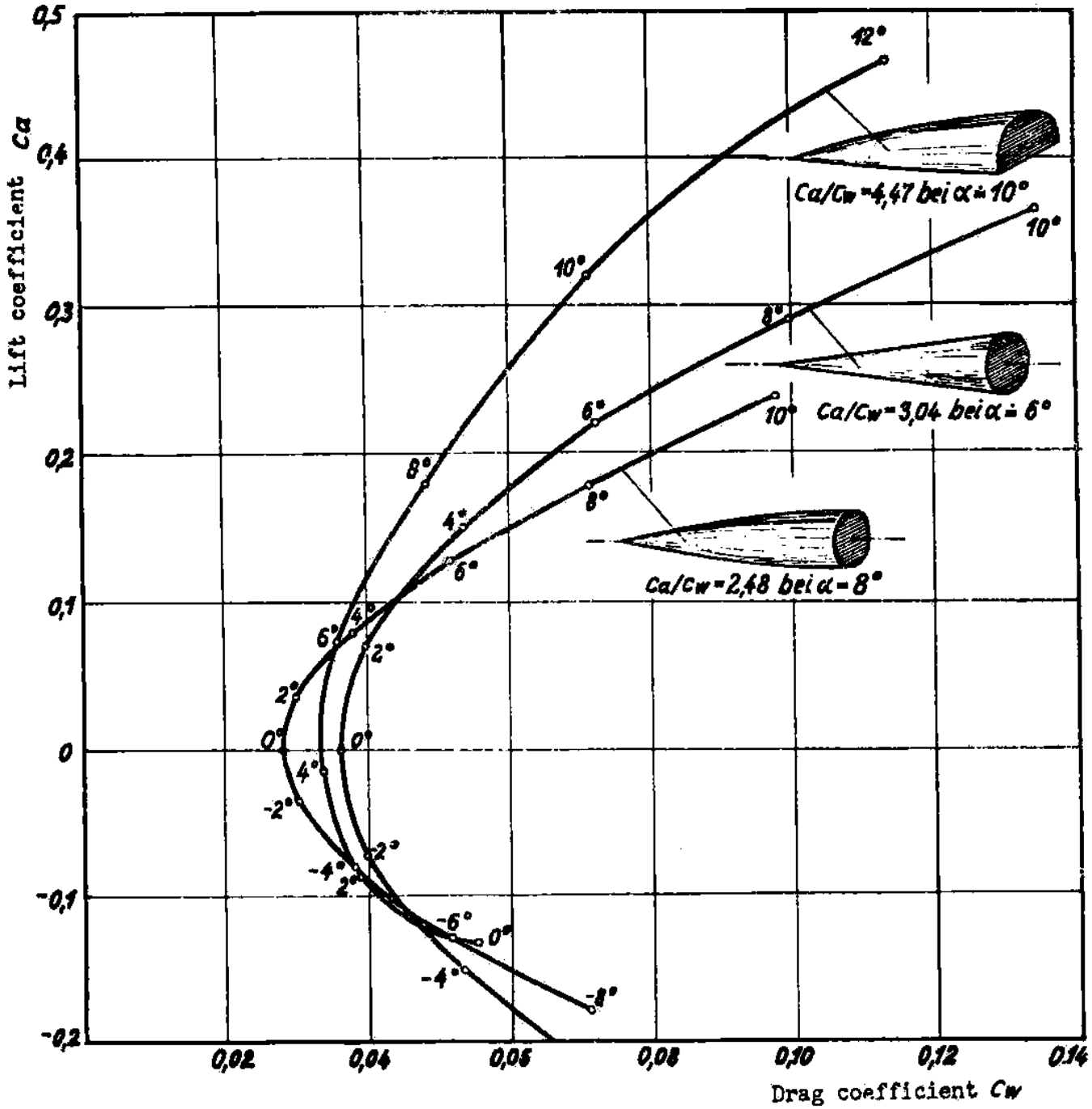

Fig. 38: Polars for three bodies having equal height and equal base cross-sectional area.

1. A right circular cone
2. An ogival shape
3. A half ogival shape

Aerodynamic coefficients are based on the base area. Mach number infinite. Gas dynamic region.

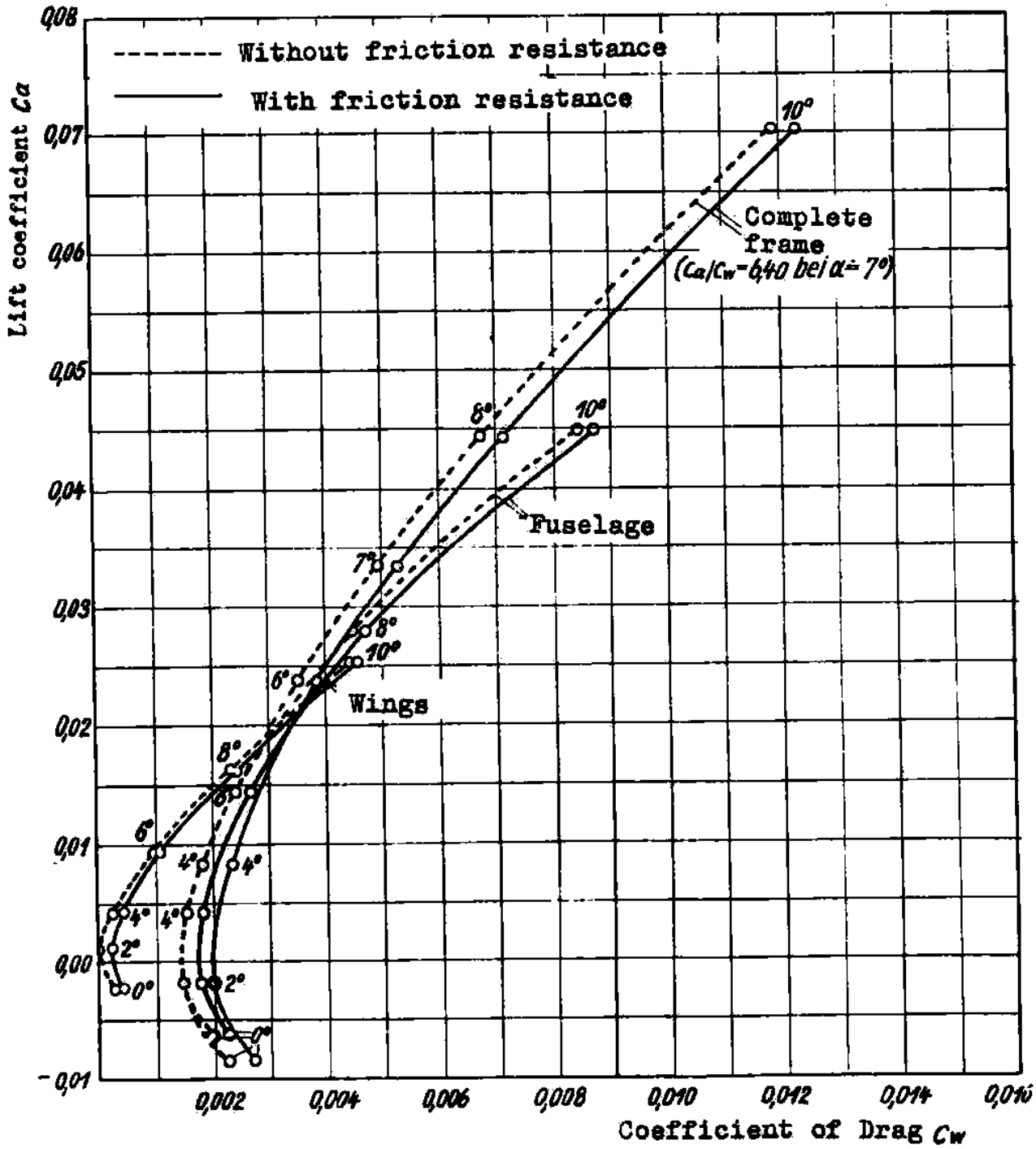

Figure 39; Computed polars of the wings, the fuselage, and the entire frame of the Rocket Bomber at M=3 (The aerodynamic coefficients are based on the area of the lifting surfaces).

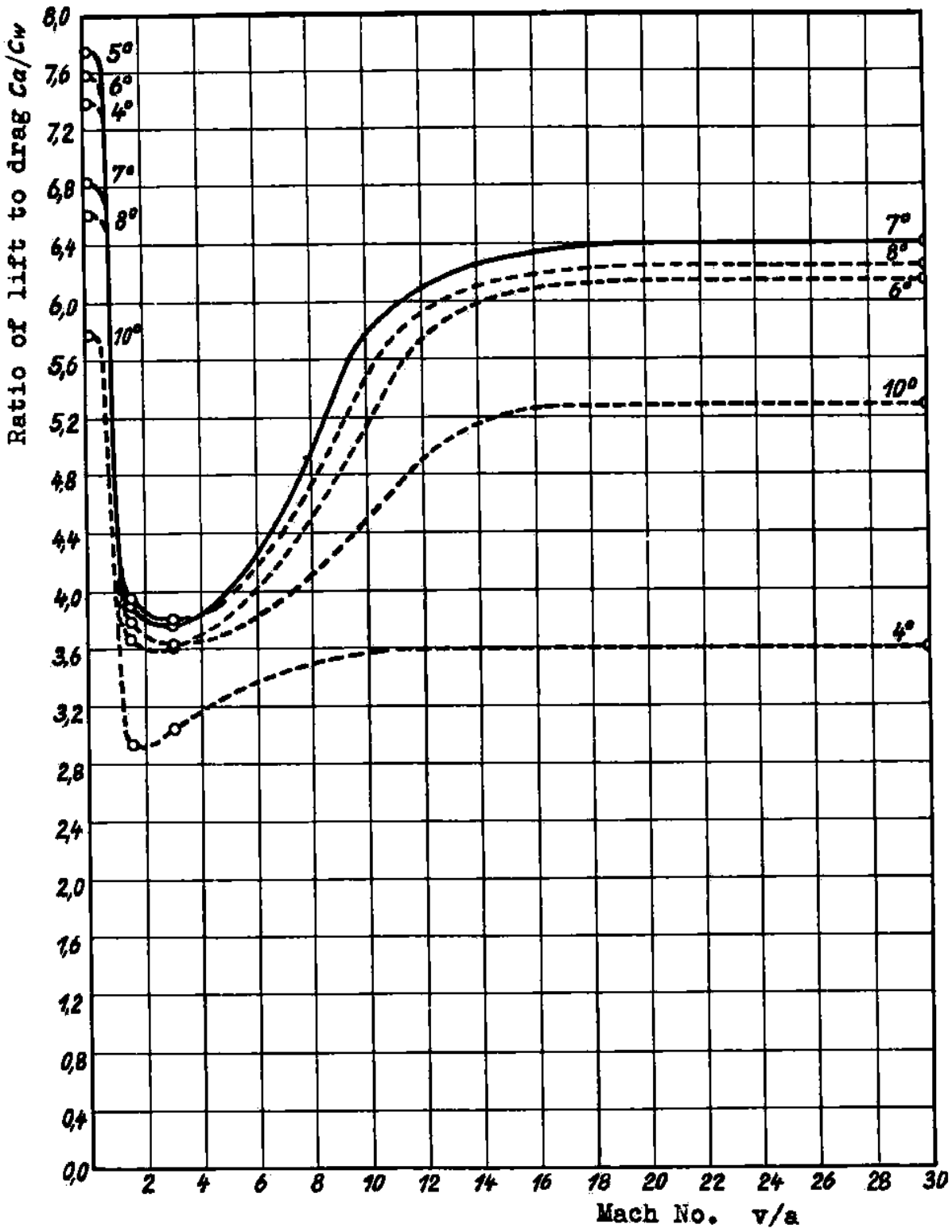

Figure 40; Probable behavior of lift-to-drag ratio and best angle of attack of Rocket Bomber at $0.1 \leq M \leq 30$.

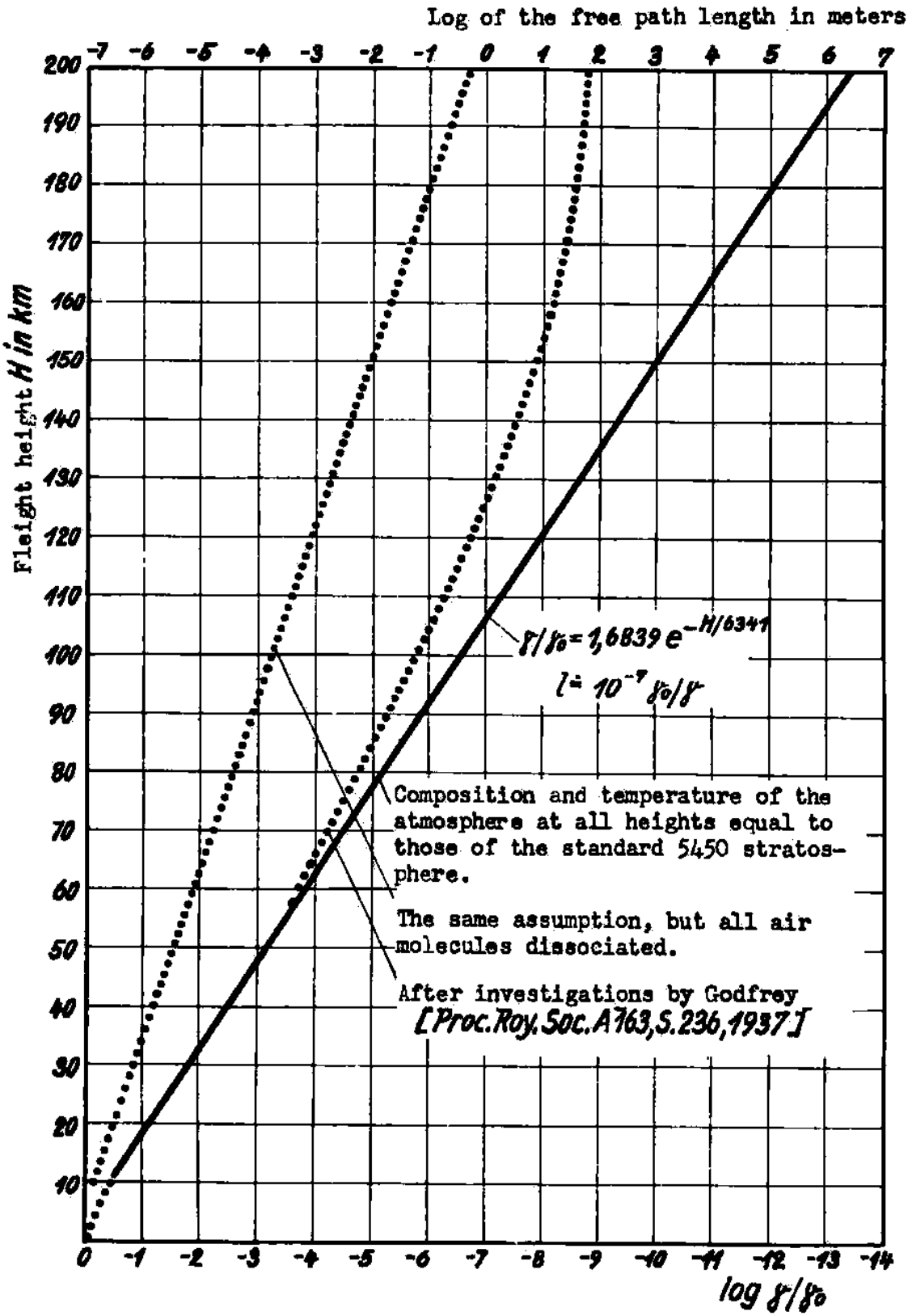

Fig. 41: Variation of the specific weight of the atmosphere, and the free path length with the flight height H.

between air molecules are already larger than the dimensions of the streams assumed in the calculation, e.g., the thickness of the boundary layer. For such rarefied air, no procedure for calculating aerodynamic forces is known. Only when, for altitudes above 100 km, the free paths approach the dimensions of the moving body, do the relations simplify sufficiently to enable a fairly exact estimate of the aerodynamic forces. (28)

In this region of gaskinetic streaming the following equations are valid for the aerodynamic forces on a body moving at arbitrary velocity V at altitudes above 100 km, where the upper (lower) sign refers to negative (positive) angles of attack:

$$p/q = (i_{pH} + i_{pR})/q$$

$$i_{pH}/q = \mp \sin\alpha \cdot \frac{C_H}{V} \cdot \frac{e^{-\frac{V^2}{C_H^2}\sin^2\alpha}}{\sqrt{\pi}} + \left(\sin^2\alpha + \frac{1}{2}\frac{C_H^2}{V^2}\right)\left(1 \mp \frac{2}{\sqrt{\pi}} \int_{x=0}^{\frac{V}{C_H}\sin\alpha} e^{-x^2} dx\right)$$

$$i_{pR}/q = +\frac{\sqrt{\pi}}{2} \cdot \frac{C_R}{V} \cdot \frac{C_H}{V} \cdot \frac{e^{-\frac{V^2}{C_H^2}\sin^2\alpha}}{\sqrt{\pi}} \mp \frac{\sqrt{\pi}}{2} \cdot \frac{C_R}{V} \sin\alpha \left(1 \mp \frac{2}{\sqrt{\pi}} \int_{x=0}^{\frac{V}{C_H}\sin\alpha} e^{-x^2} dx\right)$$

$$i_\tau/q = +\cos\alpha \cdot \frac{C_H}{V} \cdot \frac{e^{-\frac{V^2}{C_H^2}\sin^2\alpha}}{\sqrt{\pi}} \mp \sin\alpha\cos\alpha \left(1 \mp \frac{2}{\sqrt{\pi}} \int_{x=0}^{\frac{V}{C_H}\sin\alpha} e^{-x^2} dx\right)$$

where V is the speed of flight, $C_H = \sqrt{2gRT_0}$ is the most probable velocity of the gas molecules before collision with the wall, $C_R = \sqrt{2gRT_w}$ is the most probable diffuse recoil velocity of the molecules after contact with a wall at T_w°K. For very large V, i_{pH}/q approaches $2\sin^2\alpha$ (since $\int_0^\infty e^{-x^2}dx = \frac{1}{2}\sqrt{\pi}$) and i_{pR}/q approaches zero, i e. we approach the Newtonian formula $p/q = 2\sin^2\alpha$. A presentation of these aerodynamic forces in closed form as a function of Mach number is not possible; though a simple relation between C_H and a is known $C_H = a\sqrt{2/\varkappa}$, there is no corresponding relation between C_R and a.

All the equations refer to diatomic gases or gas mixtures. Also they require the knowledge of the characteristic temperature Θ, and thus involve more special assumptions than do the gas-dynamic equations which require only a knowledge of the no. of atoms per molecule and the sound-velocity, since they involve only $\varkappa$ and a.

The equations for the momentum i_{pH} of the molecules colliding with the wall, and for the tangential momentum i_τ given to the wall on recoil are taken from (28). The recoil momentum must be considered in more detail.

Before an expression for the recoil momentum can be set up, one must have a clear picture of the recoil of the molecules, which have a random thermal velocity c and a relative velocity V making an angle α with the plate. One must decide whether a bundle of molecules, striking the plate with a perpendicular velocity component $V\sin\alpha + C_x\cos\varphi$ leave the plate by specular reflection or under some other definite or random angles; further, whether the collision velocities are conserved for each individual molecule or have a definite relation to the recoil velocities, or whether they are completely random so that we can derive relations only for the average or most probable speeds, on the basis of energy considerations. One should investigate whether, during the collision, the velocities C_x as well as V are conserved, or whether they interchange their kinetic energy in whole or in part, or whether the internal degrees of freedom of the air molecules or wall molecules take part in this exchange. These questions were answered on the basis of a paper of Frenkel on "Theory of Adsorption and Related Phenomena" (4), whose opinion we give verbatim: "No matter how small the time of adherence, gas molecules colliding with a wall do not simply bounce off, but are emitted again with velocities which need not have any definite relation to the original velocity, either in magnitude or direction. The usual picture of elastic reflections of molecules, from which the kinetic theory of gases starts in deriving the pressure on the walls of the container, is false in principle. If one arrives at correct results in this case, it is because the solid body and the gas are considered to be at the same temperature and at rest relative to each other. Under these conditions, the velocity distribution of the emitted molecules is the same as if they were actually reflected from the wall surface. Actually a quite different picture would result if one bombarded the surface in a definite direction with a molecular beam." Summarizing these considerations we find that, in setting up a formula for the recoil momentum, we must consider a gas whose probable recoil velocity C_R is derivable by purely energetic considerations from the probable velocity C_H before collision, from the systematic velocity V and the wall temperature T_W. The mass of gas striking the wall per second is:

$$\bar{\rho} = \frac{\rho}{2\sqrt{\pi}} \cdot C_H \left[e^{-\frac{V^2}{C_H^2}\sin^2\alpha} + \frac{V}{C_H}\sin\alpha \left(2\int_{x=0}^{\frac{V}{C_H}\sin\alpha} e^{-x^2} dx \pm \sqrt{\pi}\right)\right] = \frac{\rho}{2\sqrt{\pi}} C_H \cdot k$$

In the normal gas-kinetic case ($V = o$ and $C_R = C_H$) the process of emission of the molecules can be considered as quasi-specular, with recoil momentum $\tau_{\rho R} = \rho C_H/4 \cdot C_H$ for a mass colliding per second of $\overline{\rho} = \frac{\rho}{2\sqrt{\pi}} \cdot C_H$. For the moving plate ($v \neq o$), K times as many molecules collide each second as for the plate at rest, and just as many must come off per second if none sticks permanently to the wall. Since according to the research cited, the process of recoil is completely independent of the process of collision, and is of the same type as for recoil at $V = o$, the only possible difference can consist in a change of the factor K for the colliding molecules $\tau_{\rho R} = \frac{\rho}{4} C_H \cdot k C_H$ as long as $C_R = C_H$. For the same reasons, the difference between recoil and collision temperatures can produce no change in the structure of the formula for the recoil momentum; one gets for $C_R \neq C_H$, $\tau_{\rho R} = \frac{\rho C_H k}{4} \cdot C_R$. The probable translational recoil speed C_R must be considered further. According to the theorem of Conservation of Energy, for the assumed closed system the sum of the energy E_R taken away by the recoiling molecules plus the energy E_W remaining at the wall must equal the energy E_A of the impinging molecules: $E_A = E_W + E_R$

$$E_A = E_{A\,trans} + E_{A\,rot} + E_{A\,osc} = A\bar{\rho}\left[\frac{v^2}{2} + \frac{C_H^2}{2}\left(\frac{3}{2} + \frac{2}{2}\right) + \frac{\theta}{T_G\left(e^{\theta/T_G} - 1\right)}\right]$$

$$E_W = E_{W\,trans} + E_{W\,rot} + E_{W\,osc} = A\bar{\rho}\left[\frac{3}{4} C_{W\,trans}^2 + \frac{1}{2} C_{W\,rot}^2 + \frac{1}{2} \frac{\theta}{T_{W\,osc}\left(e^{\theta/T_{W\,osc}} - 1\right)} C_{W\,osc}^2\right],$$

$$E_R = E_{R\,trans} + E_{R\,rot} + E_{R\,osc} = A\bar{\rho}\left[\frac{3}{4} C_{R\,trans}^2 + \frac{1}{2} C_{R\,rot}^2 + \frac{1}{2} \frac{\theta}{T_{R\,osc}\left(e^{\theta/T_{R\,osc}} - 1\right)} \cdot C_{R\,osc}\right],$$

where the values C_{rot} and C_{osc} have only a computational significance and are therefore not used in what follows.

Usually the ratio of the energy loss of the impinging molecules to the excess of their initial energy over the temperature level of the wall after collision is called the accommodation coefficient α; e.g. the average accommodation coefficient for the whole process has the value $\bar{\alpha} = (E_A - E_R)/(E_A - E_W)$. The accommodation coefficients for the individual degrees of freedom can be written as:

$$\alpha_{trans} = (E_{A\,trans} - E_{R\,trans})/(E_{A\,trans} - E_{W\,trans}) = \left(V^2 + \frac{3}{2} C_H^2 - \frac{3}{2} C_{R\,trans}^2\right)/\left(V^2 + \frac{3}{2} C_H^2 - \frac{3}{2} C_{W\,trans}^2\right)$$

$$\alpha_{rot} = (E_{A\,rot} - E_{R\,trans})/(E_{A\,rot} - E_{W\,rot}), \quad \alpha_{osc} = (E_{A\,osc} - E_{R\,osc})/(E_{A\,osc} - E_{W\,osc})$$

The average accommodation coefficient $\bar{\alpha}$ is built up from the coefficients for the separate degrees of freedom as follows:

$$\bar{\alpha} = \alpha_{trans}(E_{A\,trans} - E_{W\,trans})/(E_A - E_W) + \alpha_{rot}(E_{A\,rot} - E_{W\,rot})/(E_A - E_W) + \alpha_{osc}(E_{A\,osc} - E_{W\,osc})/(E_A - E_W)$$

Considerations on accommodation coefficients in the physical literature state in essence that the external degrees of freedom take part immediately and completely in the energy exchange during molecular processes, whereas the exchange of internal molecular energy, especially that of vibration, is slowed down considerably and is effective only after long relaxation times, so that the accommodation coefficients for translation are 1 and also α_{rot} may be assumed to be ≈ 1, while the deviations of the total accommodation coefficient $\bar{\alpha}$ from 1, observed in practice, are to be ascribed to the slowness of changes in vibration. From $\alpha_{trans} = 1$ it follows that $C_{R\,trans} = C_{W\,trans} = \sqrt{2gRT_W}$ where $C_{R\,trans}$ is thus the desired most probable recoil velocity of the molecules leaving the wall diffusely; T_W is the wall temperature in °K.

Before calculating the aerodynamic forces one must estimate the wall temperature T_W. This is done by equating the energy radiated by the wall per cm^2 per sec. $E_S = \varepsilon_a \frac{4.96}{3600}\left(\frac{T_W}{100}\right)^4$ to the energy E_W transferred by the air molecules to the same surface in the same time. If one introduces the previously established assumptions $\alpha_{trans} = 1$, $\alpha_{rot} = 1$, $\alpha_{osc} = 0$, one obtains $E_W = A\bar{\rho}\left[\frac{v^2}{2} + \frac{5}{2} gR(T_G - T_W)\right]$ where $\bar{\rho}$ is the mass of the molecules striking unit area of the plate per unit time. These expressions were used in constructing Fig. 42, where the following numerical values were assumed; temperature of still air $T_G = 320$ °K, density of still air $\rho = 10^{-7}\,kg\,sec^2/m^4$, (corresponding to H ≈ 90 km.) composition of the air 14% O_2 + 86% N_2. Ionization and dissociation were not considered; also the atmosphere was assumed to be at rest on the earth's surface. The optical absorption of the wall was assumed to be $\varepsilon_a = 0.80$. Radiation of heat to the wall from the outside (sun), from the air space or the earth's surface was neglected, as well as from the interior of the aircraft to the wall. Fig. 42 shows that the equilibrium temperature of the plate at rest is 136° K and that this equilibrium temperature of the surface of the aircraft increases with increasing velocity and angle of attack, as long as the latter is positive so that the surface is tilted toward the course wind. For surfaces to leeward the equilibrium temperature drops to absolute zero, since the heat supply vanishes with the number of impinging molecules. Altogether the temperatures remain within reasonable limits for all angles of attack and velocities occurring in practice. At greater heights even lower temperatures may be expected; at lower heights a transition occurs to temperatures calculable by kinetic theory.

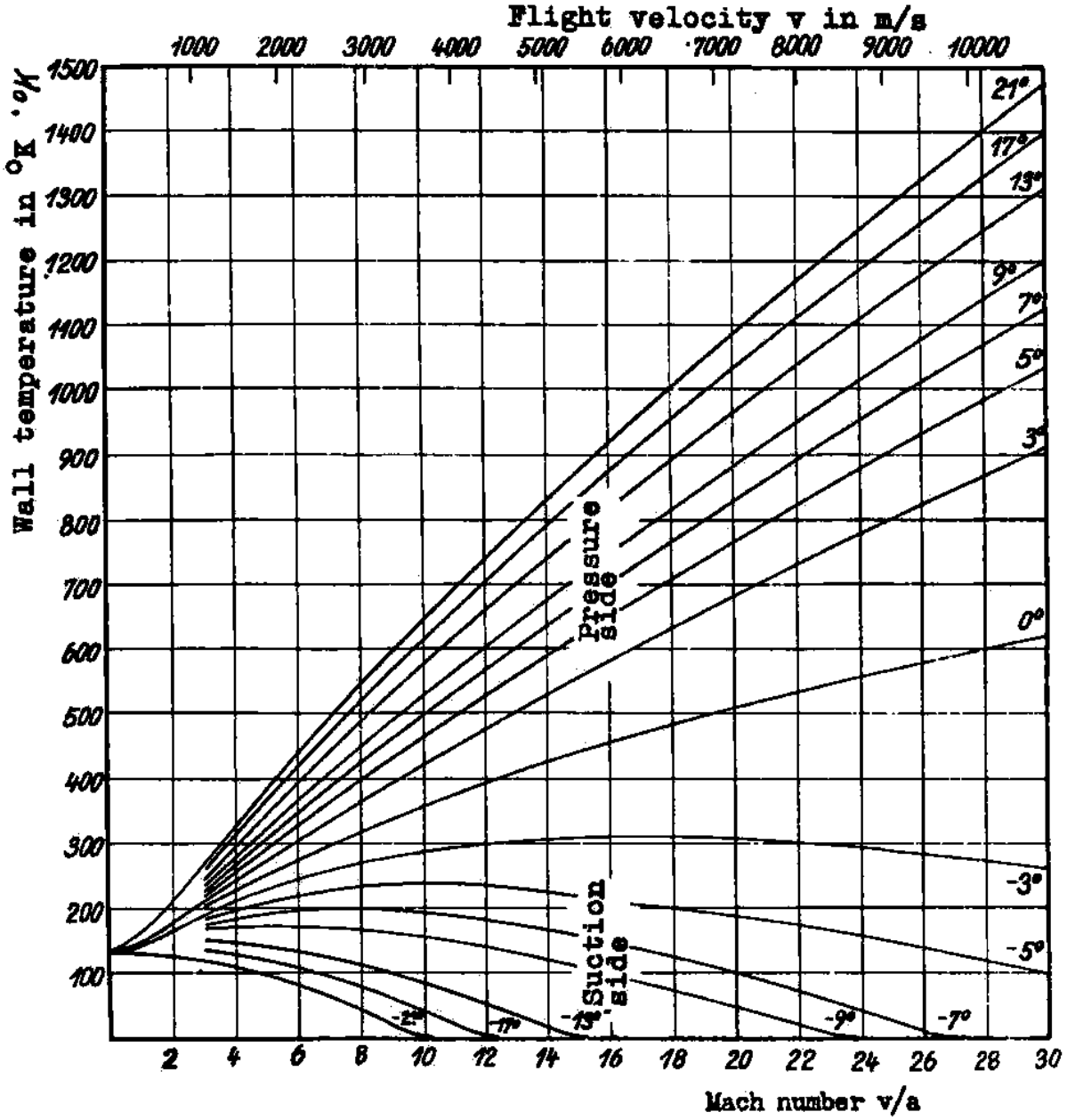

Fig. 42: Surface temperature of a flat plate in an atmosphere of 86% N_2 and 14% O_2 and with density $\rho = 10^{-7}$ kg sec^2/m^4 (in molecular flow region) for various flight velocities v/a and various angles of attack α

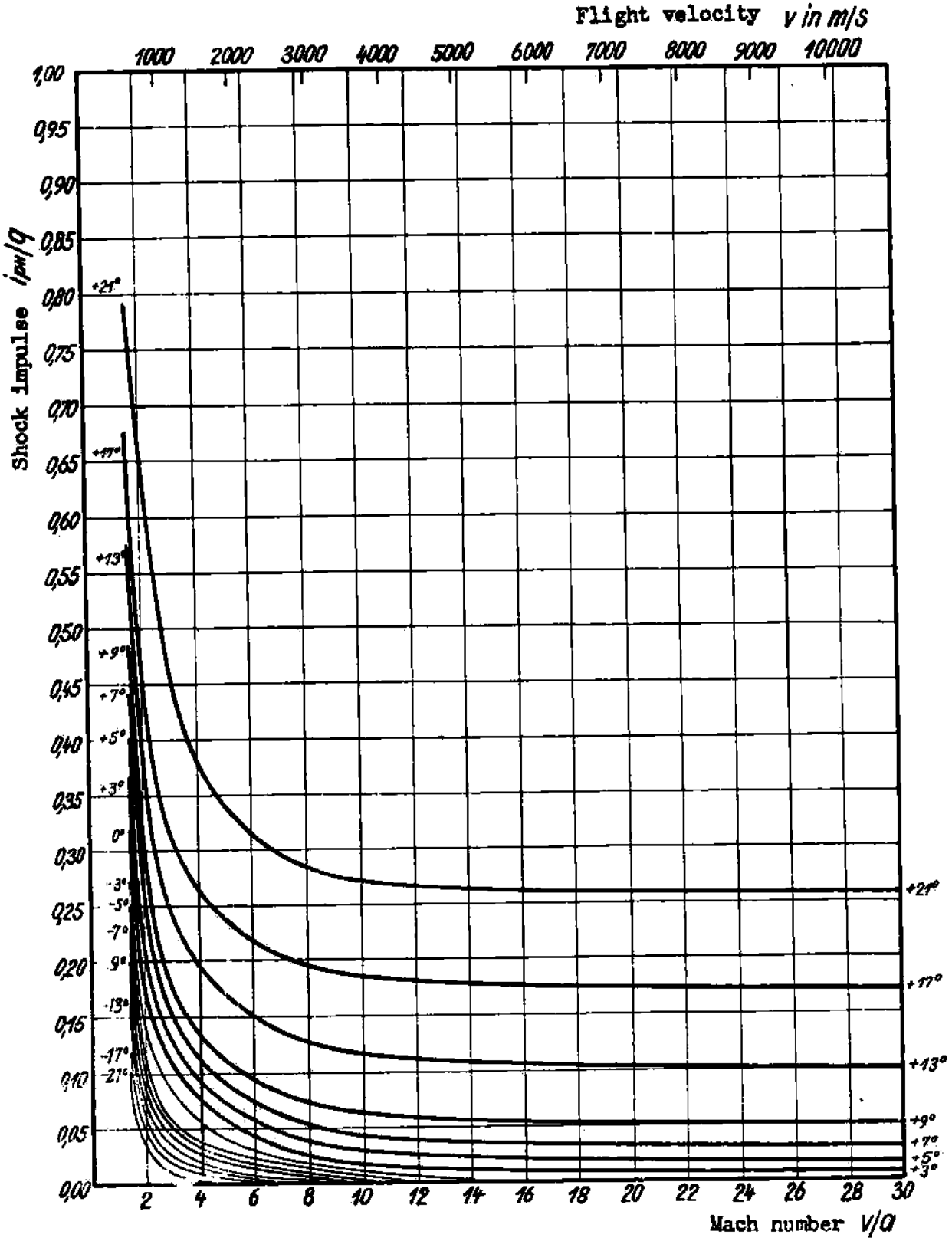

Fig. 43: Coefficients iph/q of a shock impulse perpendicular to a flat plate for various flight velocities v and angles of attack α in an atmosphere of 86% N_2 and 14% O_2 and density $\rho = 10^{-7}$ kg sec^2/m^4 (molecular flow region).

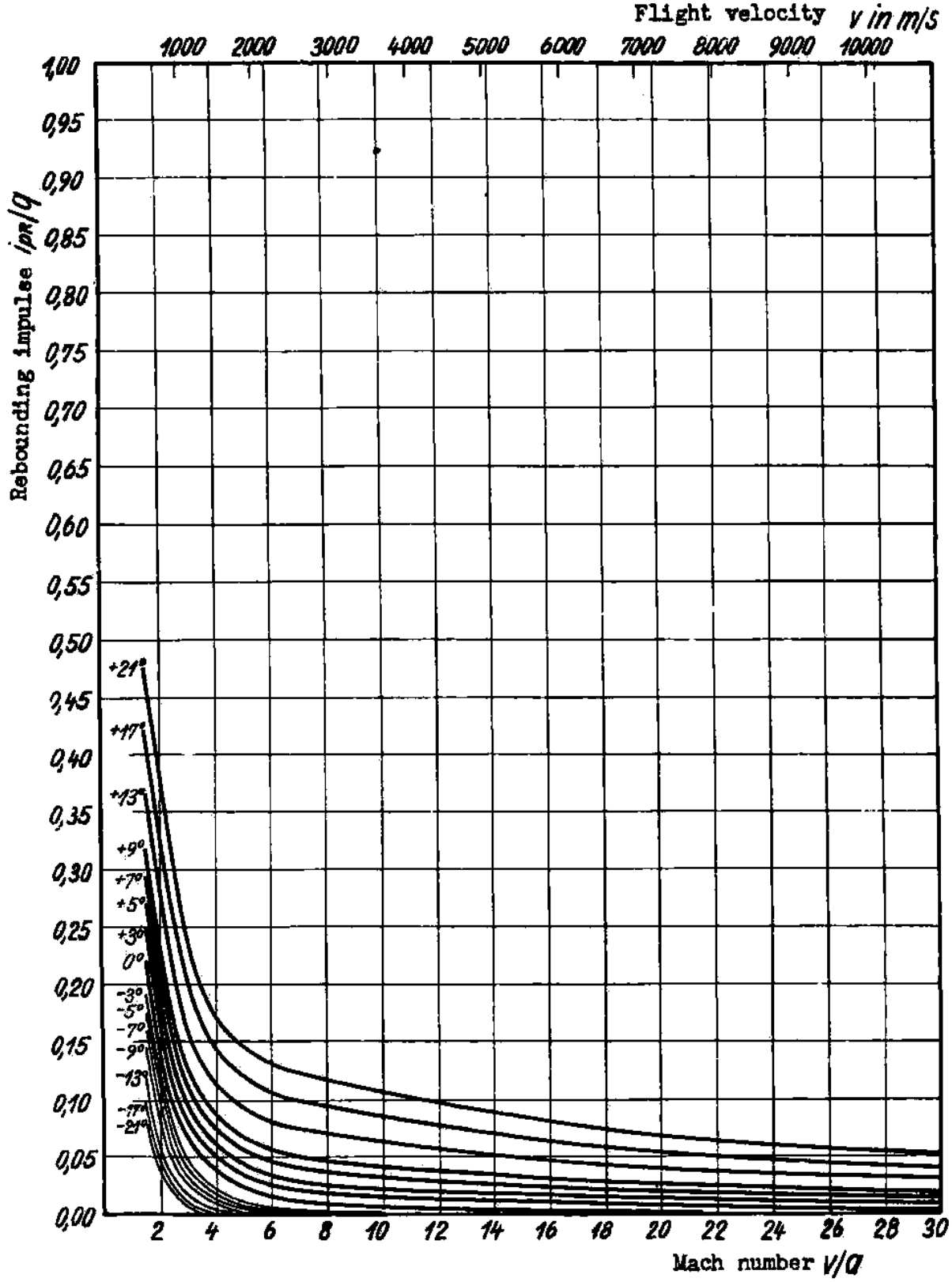

Fig. 44: Coefficient ipR/q of restitution (rebounding impulse) on a flat plate for various flight velocities v and angles of attack α in an atmosphere of 86% N_2 and 14% O_2 and density $\rho = 10^{-7}$ (molecular flow region).

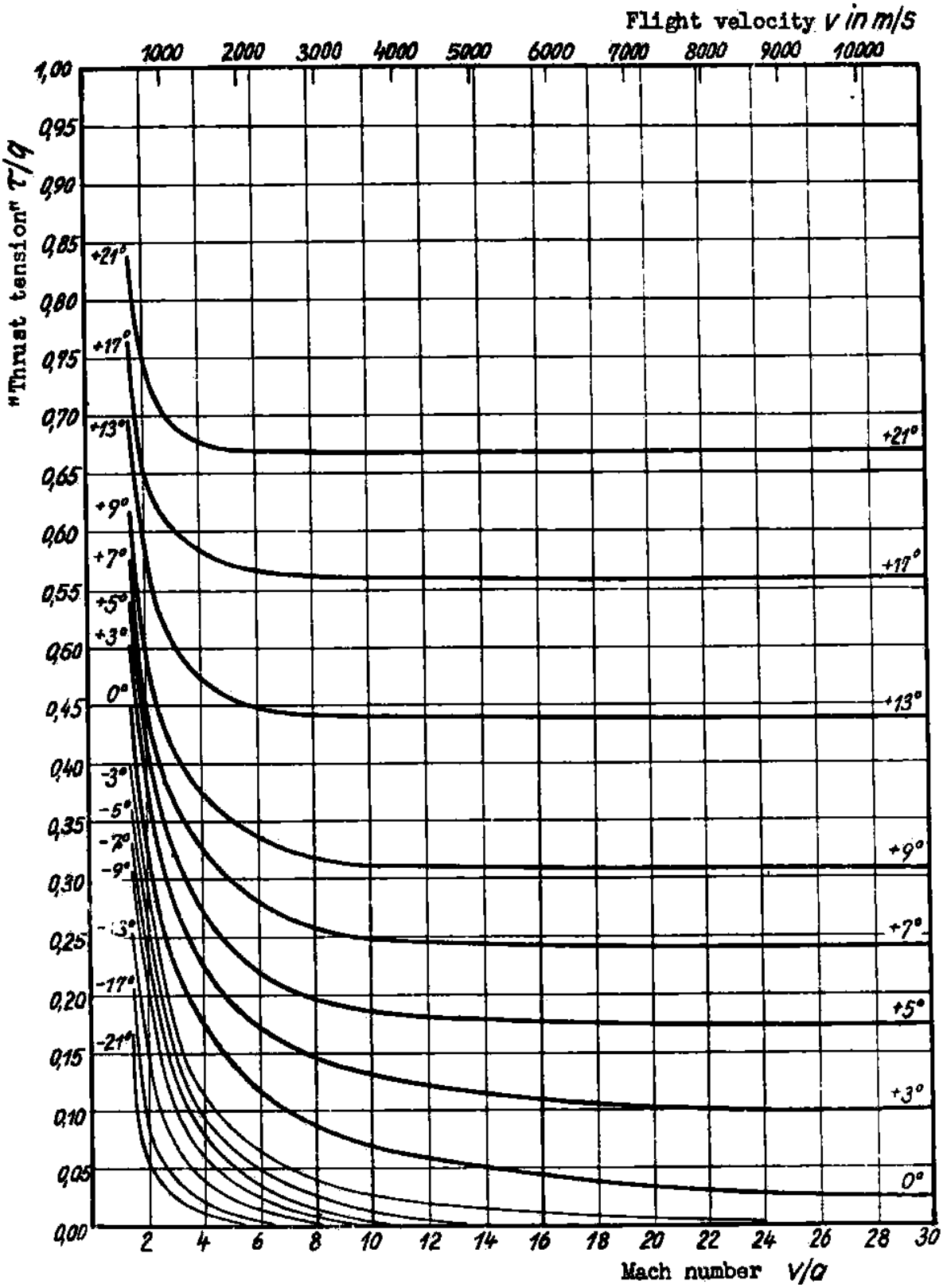

Fig. 45: Coefficient τ/q of the thrust tension between air and plane plates for various flight velocities v and various angles of attack α in an atmosphere of 86% N_2 and 14% O_2 and density $\rho = 10^{-7}$ kg sec^2/m^4 (molecular flow region).

With the aid of the equations the aerodynamic forces were calculated for an assumed atmosphere with temperature 320° K, density 10^{-7} kg sec^2/m^4 and composition 14% O_2 + 86% N_2. The momentum i_{pH} of the air impinging on the plate is plotted in Fig. 43 for various angles of attack and velocities of flight; the corresponding recoil momentum i_{pR} is shown in Fig. 44, and the tangential momentum in Fig. 45. Since $i_T = \tau$, Fig. 45 also represents the coefficient of friction τ/q between the air and the wall, for all angles of attack and for the same range of flight velocities. In this figure, the extraordinarily large coefficient of friction in the domain of gas-kinetic streaming is noteworthy. While values of τ/q = 0.001 to 0.003 are customary in aerodynamics, we have in this case values of the friction 300 to 1000 times as large, and these are not accompanied by corresponding increases in the values of the perpendicular components of the aerodynamic forces. The reason for this astonishingly high friction is the fact that in the domain of gas-kinetic streaming the protective boundary layer at the surface of the moving body no longer exists, so that all the molecules which have the chance to transfer perpendicular momentum to the wall, at the same time transfer their tangential momentum completely on the average, whereas this latter momentum transfer is limited to the few molecules inside the boundary layer, in the case of aerodynamic streaming. This very unfavorable behavior of the aerodynamic forces in the rare upper atmosphere would completely prevent flight at these heights, if the stagnation pressures and consequently the forces did not decrease rapidly and finally vanish. Obviously the shaping of the aircraft to fit the streaming conditions loses some of its significance of these heights. Nevertheless, the Newtonian character of the air pressures (i.e. their quadratic dependence on flight velocity and angle of attack), and the rapid disappearance of forces on leeward surfaces, is very apparent at higher velocities of flight. Thus in the gas-kinetic domain all the requirements are fulfilled for the use of streamlined bodies, whose underside is curved as little as possible in the direction of streaming, and whose upper side consists, as far as possible, of leeward or convex surfaces, while the thickness of the body is of no importance. Reciprocal streamline-numbers and polars were derived for the flat plate, from Figs. 43-45, and plotted in Figs. 46 and 47. These graphs of the behavior of the aerodynamic forces on a flat, infinitely thin plate, have direct practical importance, because any wing profile of finite thickness, with a flat under-side and upper-side to leeward, undergoes exactly these same aerodynamic forces at high flight velocities, regardless of the shape of the upper side and the thickness of the profile.

Figs. 48 and 49, which show the aerodynamic-forces on the rocket bomber in the range of gas-kinetic streaming, were also derived from Figs. 43-45. In the same way as for the gas-dynamic calculations, the actually curved surface of the aircraft was split up into a number of small flat surfaces, and the air forces calculated for each of these component surfaces.

Finally Fig. 50 shows a plot of the dependence of the air forces on height and velocity of flight for the domains of gas-dynamic and gas-kinetic streaming. This plot of ρ/q against height, for the flat plate, for various Mach numbers and with the fixed angle of attack of 7° (which is the optimum for the gas-kinetic case), shows that the air-force-coefficients decrease with height in this region. This phenomenon is caused by the decrease of temperature of the plate with height, so that ceteris paribus the recoil velocity and recoil momentum also decrease. The forces in the range of heights from 40-90 km (which cannot be calculated exactly) were interpolated approximately in the form of the dotted curve.

Fig. 51 shows the final result of this whole section, i.e. the dependence of the rocket bomber's glide number (or its reciprocal) on the velocity and altitude of flight. With this we close the investigations on glide-number of the rocket bomber.

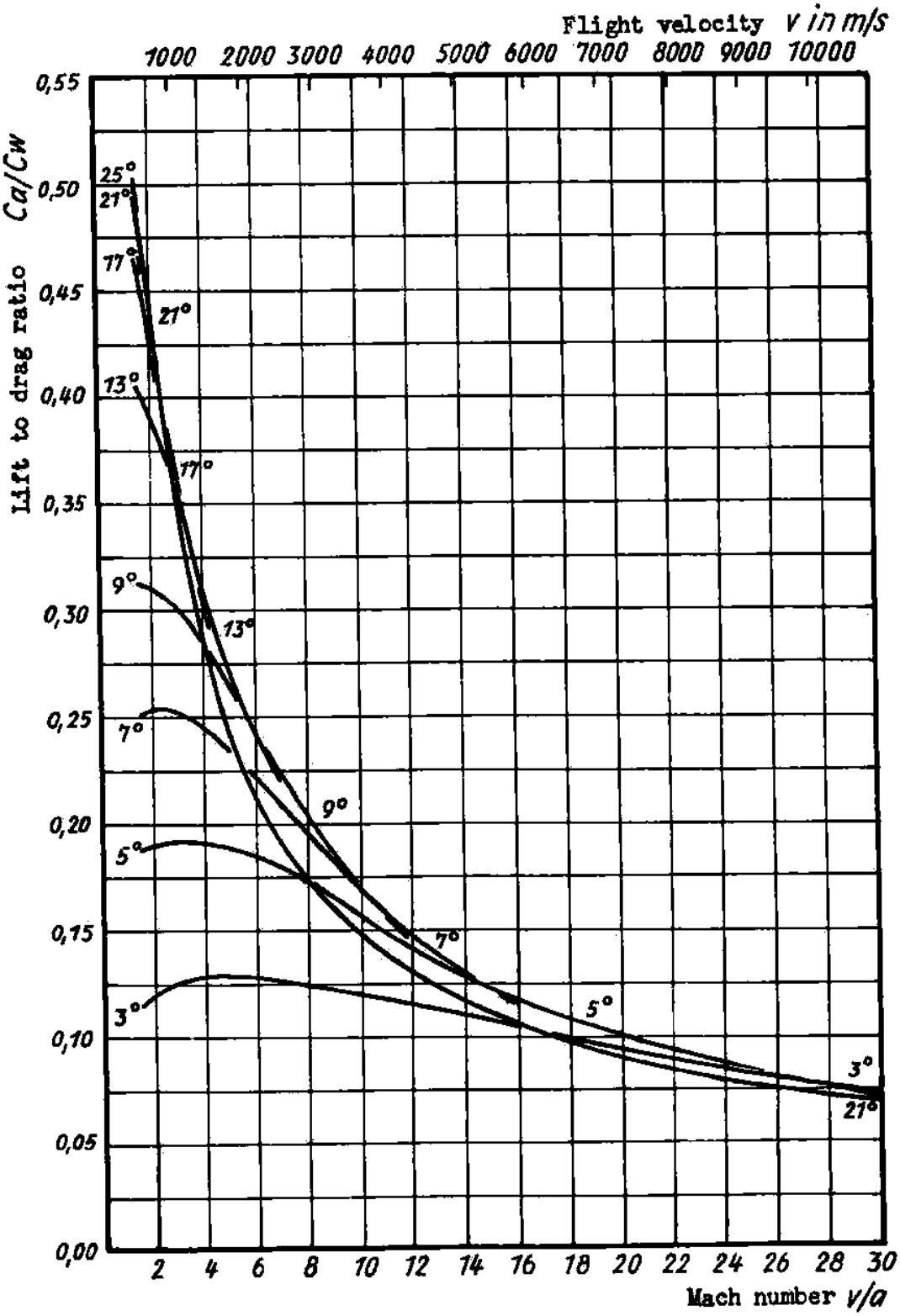

Fig. 46: Lift to drag ratio of a flat infinitely thin plate in molecular flow region.

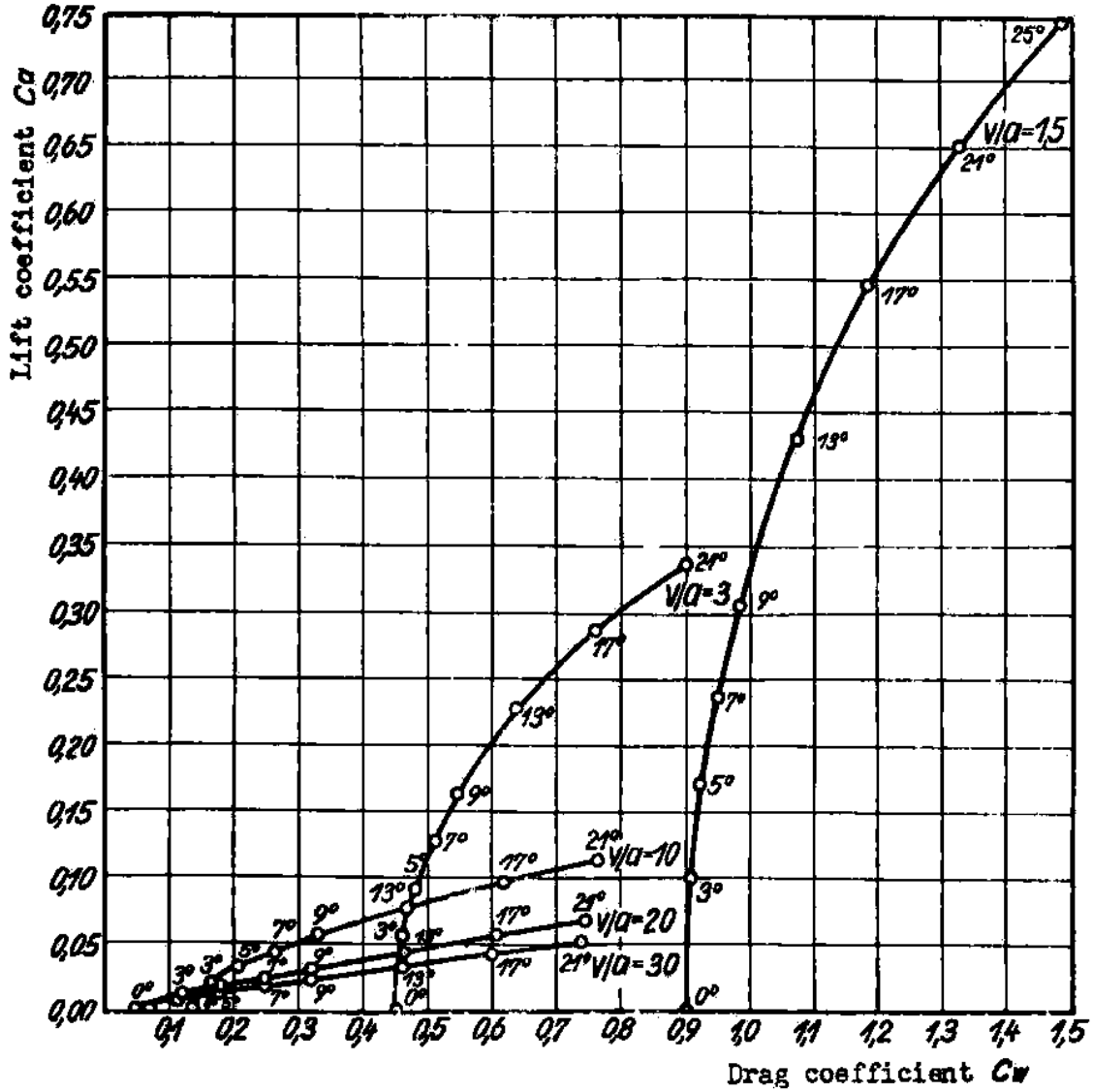

Fig. 47: Polars of a flat, infinitely thin plate in molecular flow region for various flight speeds.

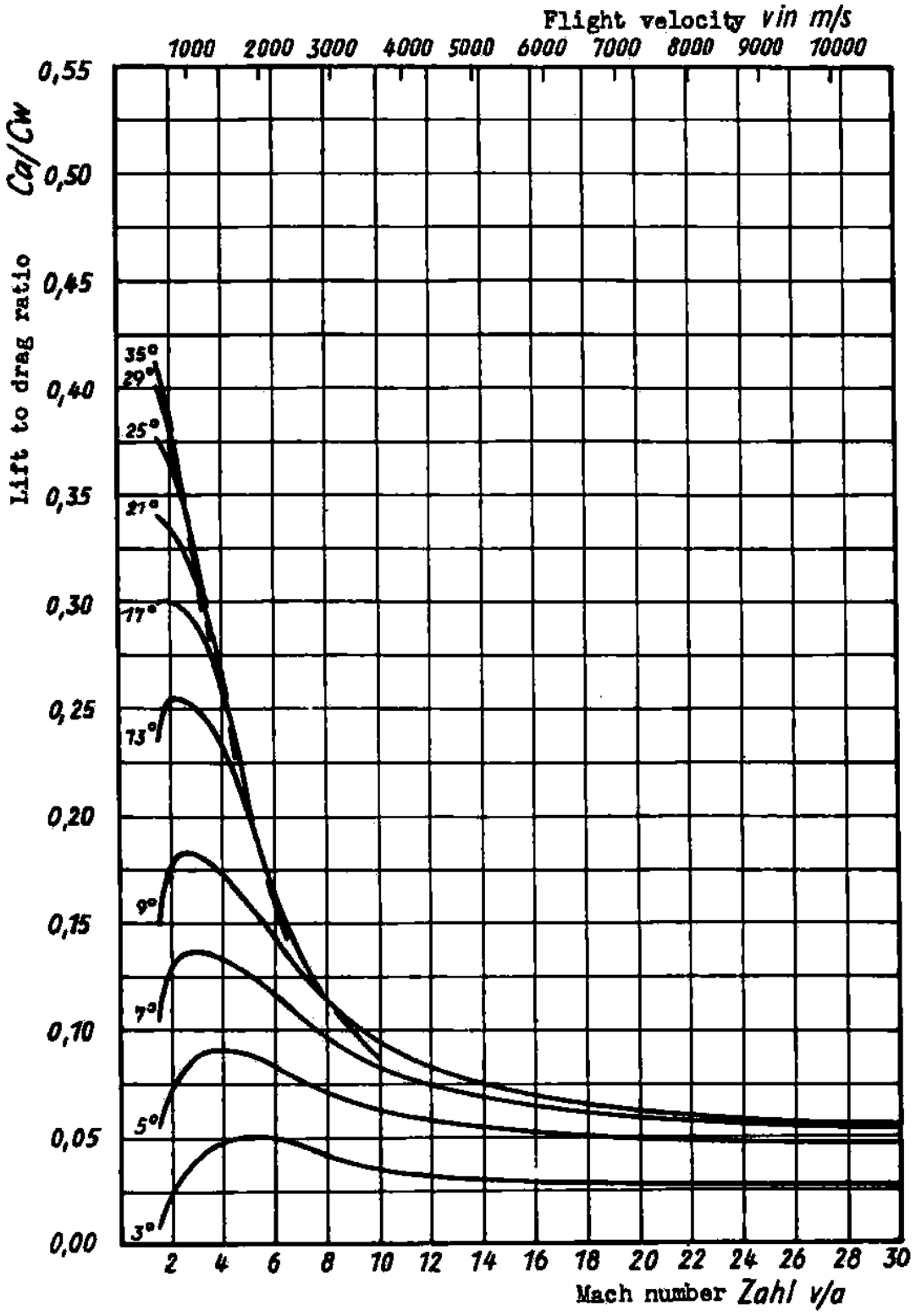

Fig. 48: Lift to drag ratio of the Rocket Bomber in molecular flow region.

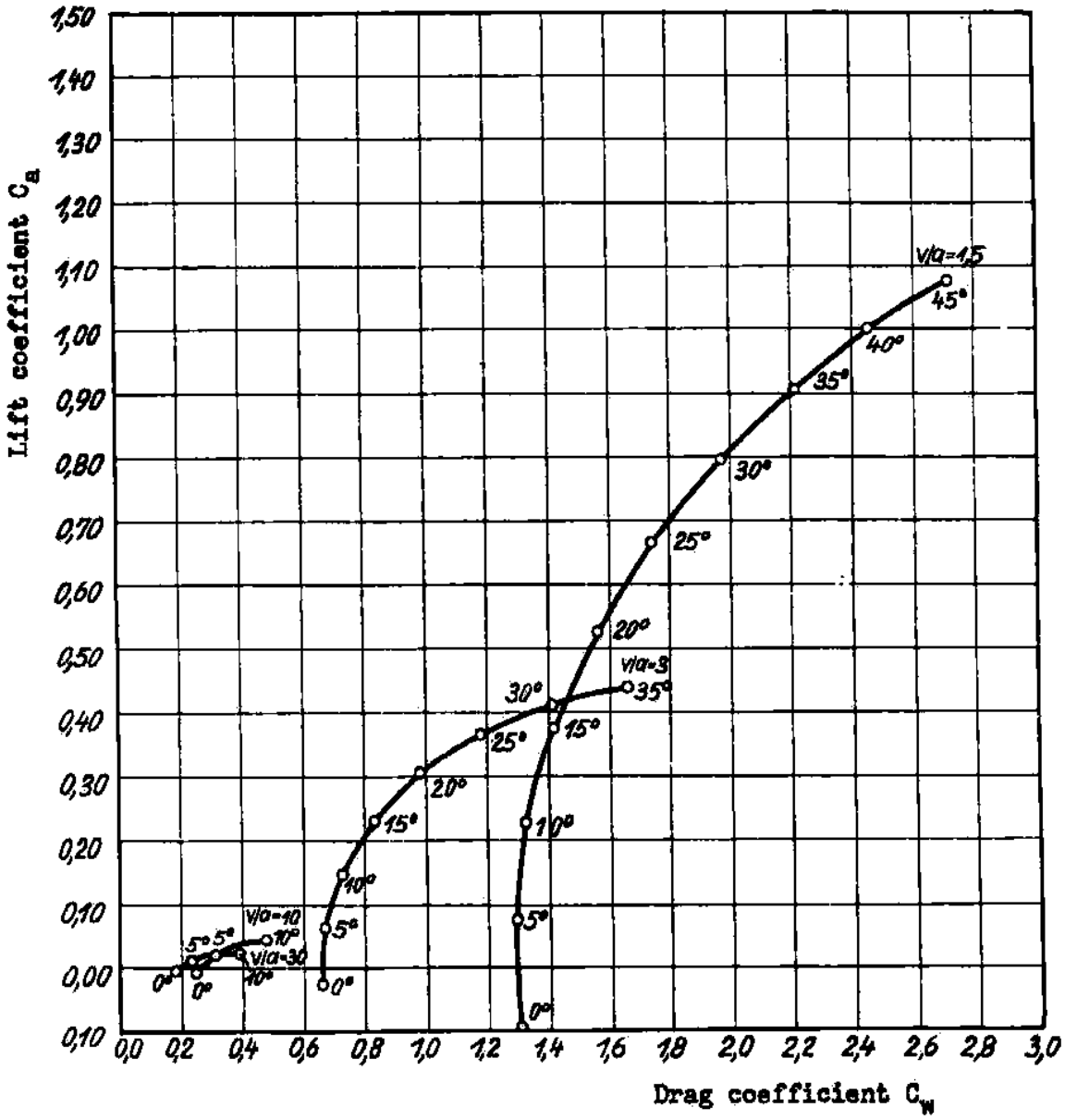

Fig. 49
Polars of the Rocket Bomber in the molecular flow region for various flight velocities.

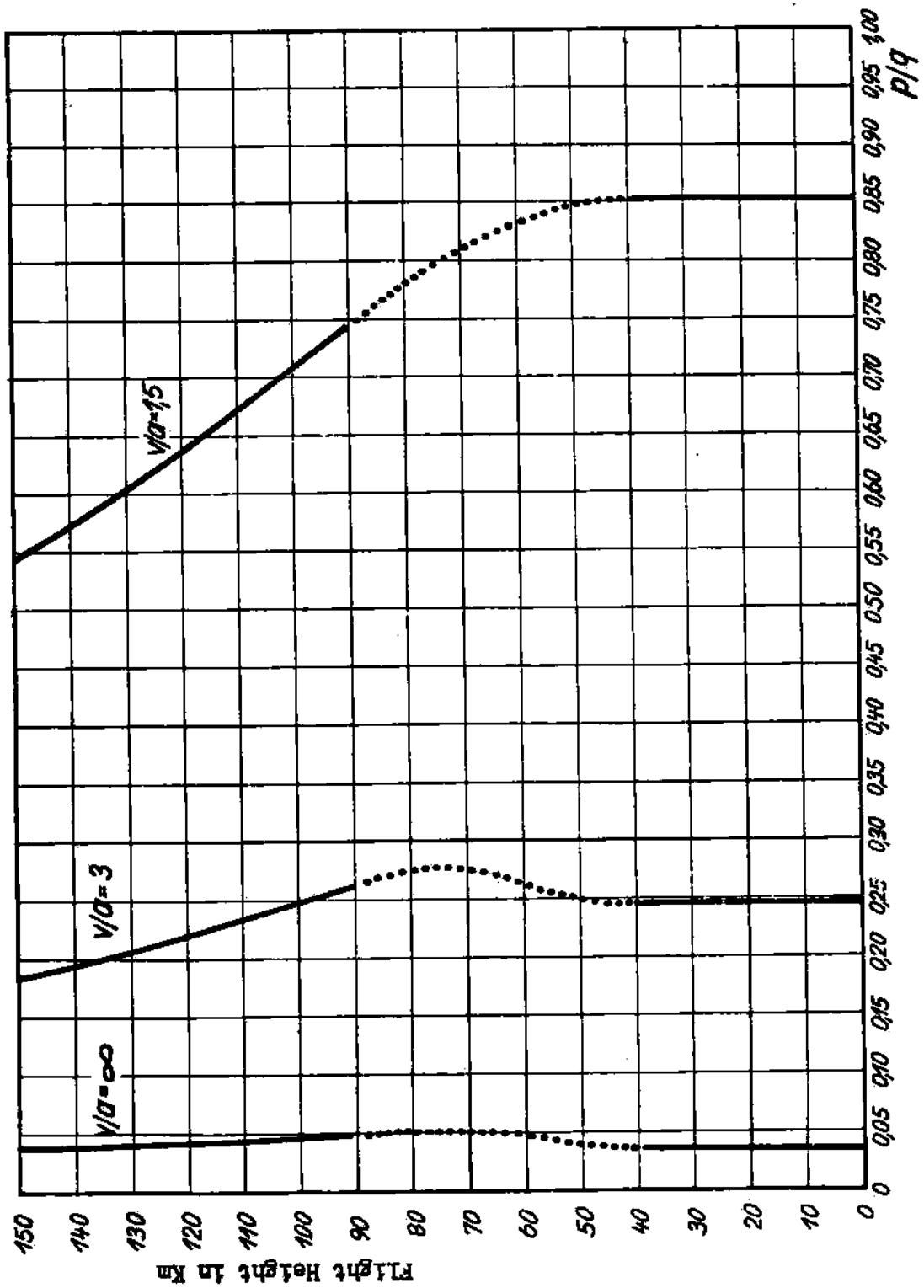

Fig. 50; Behavior of the coefficient $p/_q$ of the air pressure perpendicular to a flat plate when angle of attack $\alpha = 7^\circ$ as a function of flight velocity and flight altitude (conventional fluid mechanics, molecular flow, and transition region).

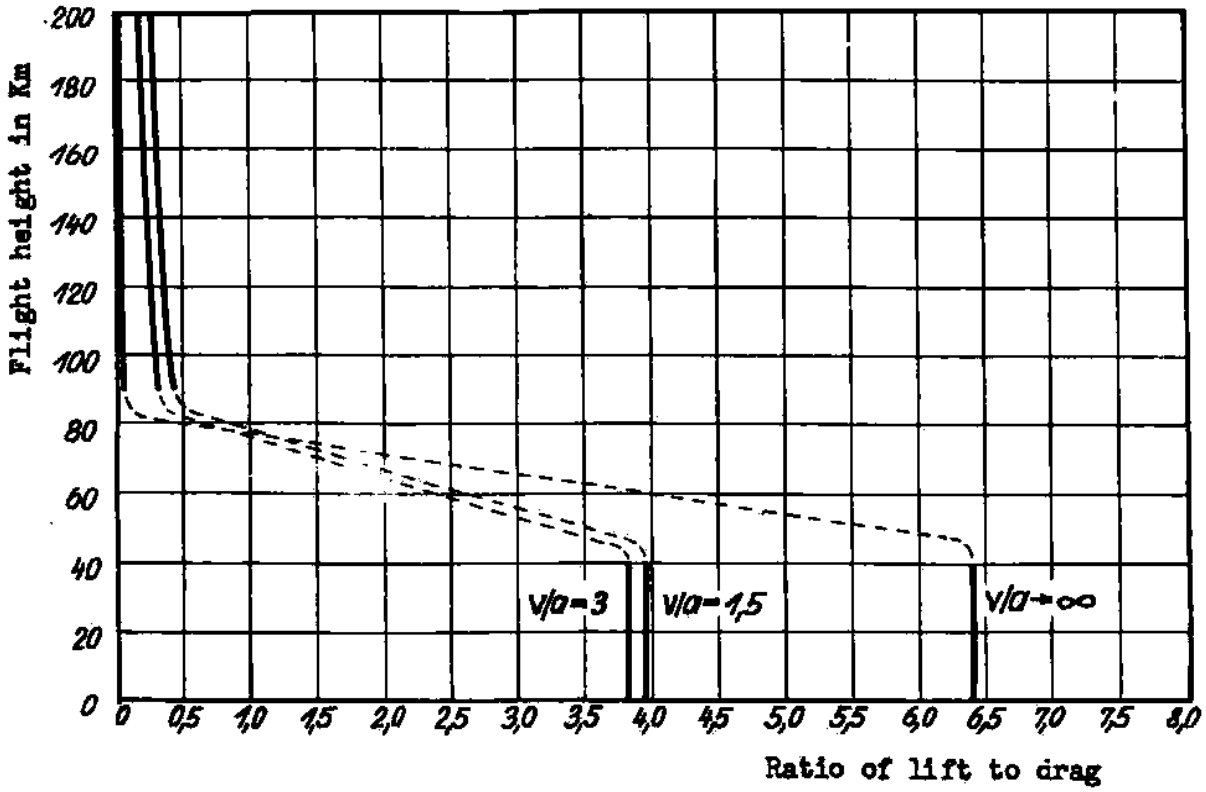

Fig. 51;

Behavior of the best lift to drag ratio of the Rocket Bomber plotted against the flight altitude and flight velocity (conventional fluid mechanics, molecular flow, and transition region).

III. LAUNCHING AND CLIMB

1. Acceleration of the Aircraft

The launching and climb of the rocket bomber have the purpose of giving it, with a minimum of fuel consumption, the high velocity necessary to carry it through its long glide path; they are in the nature of an impulse which lasts only for a few minutes. Despite this, there are various possibilities for the variation of this external force during this short time; we wish to find the most favorable, i. e., the one with the least possible fuel consumption for a given final velocity.

In Fig. 52, the effective exhaust speed c is again taken as a measure of the useful energy content per unit mass of fuel and the attainable velocity increase V is measured in units of c; the fuel consumption $G_o - G$ is measured in units of the starting weight G_o or the weight of the accelerated mass G. If one could completely transfer to the accelerating body the energy available from the combustion gases $(G_o - G)c^2/2g$, which is theoretically possible in firing from a tube, then $V/c = \sqrt{G_o/G - 1}$. This relation for ideal fire is shown as curve 1 in Fig. 52. In the case of rocket drive, the acceleration process, if it was opposed only by the inertial forces of the bomber and not by air resistance, gravity, etc., would after integration of the equations expressing the Conservation of the Center of Mass ($c\,dm + m\,dv = 0$), be represented by the fundamental rocket equation $V/c = \ln G_o/G$. Curve 2 for ideal rocket acceleration thus gives much smaller final speeds for the same fuel consumption. The energy lost to the acceleration process is that of the motion of the combustion gases relative to the place of launching; this is often called the external efficiency of the rocket drive. This fundamental curve for ideal rocket drive gives no indication of the actual accelerations. Actually the acceleration of the bomber occurs against air resistance and at least a component of the weight and these resistances become more important for the smaller accelerations. For example, if one assumes that the air resistance and the component of weight along the path together represent a fixed fraction, say 1/5, of the instaneous weight and that the acceleration is constant during the climb, then one can denote by k the ratio of the rocket thrust reduced by the resisting forces to the effective thrust; from the equation $kc\,dm + m\,dv = 0$, one then derives a modified rocket equation $V/c = k \ln G_o/G$. If one takes the rocket thrust to be equal to the instaneous weight, then $k = (1 - 0.2)/1 = 0.8$ and the curve for this type of drive has the equation $G/G_o = e^{V/0.8c}$ or $V/c = 0.8 \ln \frac{G_o}{G}$. This curve for K = 0.8 is shown as number 3 in Fig. 52. In practice one does not obtain this curve if the aircraft starts with customary small speed at the ground, because for the assumed accelerations the aerodynamic forces would increase much too quickly for subsonic velocities. Curve 4 shows the climbing process for a commercial rocket plane with high requirements of safety and convenience, i.e., small takeoff and landing speeds, and small, practically constant accelerations along the path of climb; these are taken from a previous detailed calculation of the path. (18) The long, tedious, uneconomical climb until the velocity of sound is reached is shown clearly; we see how costly low velocities at the ground and the accompanying small accelerations are for rocket flight. Curve 5 shows a possible acceleration process under the following assumptions: the rocket thrust is a times the initial weight G_o and stays constant over the whole path of climb; thus the acceleration increases with the decreasing mass of the rocket up to a value determined by the weight of the crew and the aircraft, and the rocket motor is used fully. Thus the weight loss per second is constant and equal to $a G_o \cdot g/c$ so that the weight at time t is: $G = G_o(1 - agt/c)$. By equating the inertial and friction forces (the latter with the same assumptions as for curve 3) to the rocket thrust, it follows that $V/c = \ln G_o/G - 0.2(1 - G/G_o)/a$. This calculation is shown in Fig. 52 for three values of a, P/G_o = 0.25, 1.0 and 10. In the curve for $P/G_o = 0.25$ the acceleration increases from 0.5 m/sec^2. to 25 m/sec^2. Because of the small acceleration the curve deviates noticeably from that for ideal rocket drive. For the case $P/G_o = 1.0$, in which thrust and initial weight are equal, the accelerations vary between 10 m/sec^2 and 100 m/sec^2, and the curve approaches most closely that for ideal rocket drive. Finally for $P/G_o = 10$, the thrust is ten times the initial weight, the accelerations lie between 100 m/sec^2 and 1000 m/sec^2, which is certainly way beyond humanly bearable limits. Thus the very great effect of the acceleration process on the final velocity attainable with a given G/G_o is clear.

The curves for $P/G_o = 1$ and 10 are based on such reasonable assumptions that noticeably more favorable types of launching could hardly be found; thus more detailed study of the processes of takeoff and climb under these assumptions is advisable. The two curves differ only in the accelerations during the climb. The usable accelerations are limited only by the strength of the aircraft and by human resistance. From our present knowledge of the physiological behavior of the man under high accelerations one must admit that an unmanned rocket aircraft can be driven at somewhat higher accelerations than a manned craft; nevertheless, the unmanned craft also soon reaches the point where greater accelerations are compensated for by the greater construction weight necessary for craft capable of undergoing large accelerations. In addition the rocket

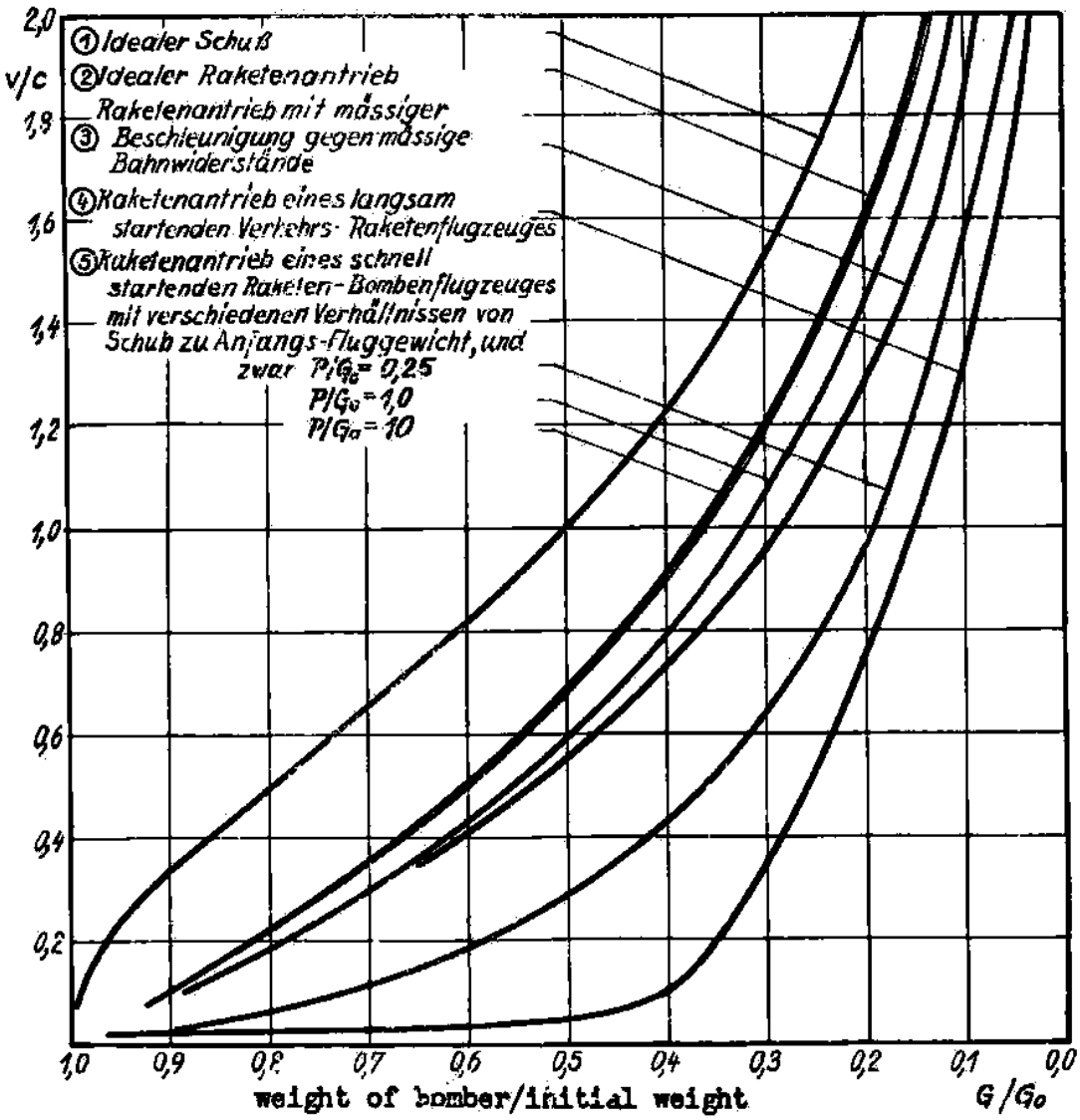

Fig. 52; Reference curves for the Rocket take-off.

(1) Ideal trajectory "shot"
(2) Ideal rocket take-off
(3) Rocket take-off with moderate acceleration against moderate path resistance
(4) Rocket take-off of a slowly starting commercial rocket plane
(5) Rocket take-off of a rapid starting rocket bomber with various ratios of thrust to initial weight

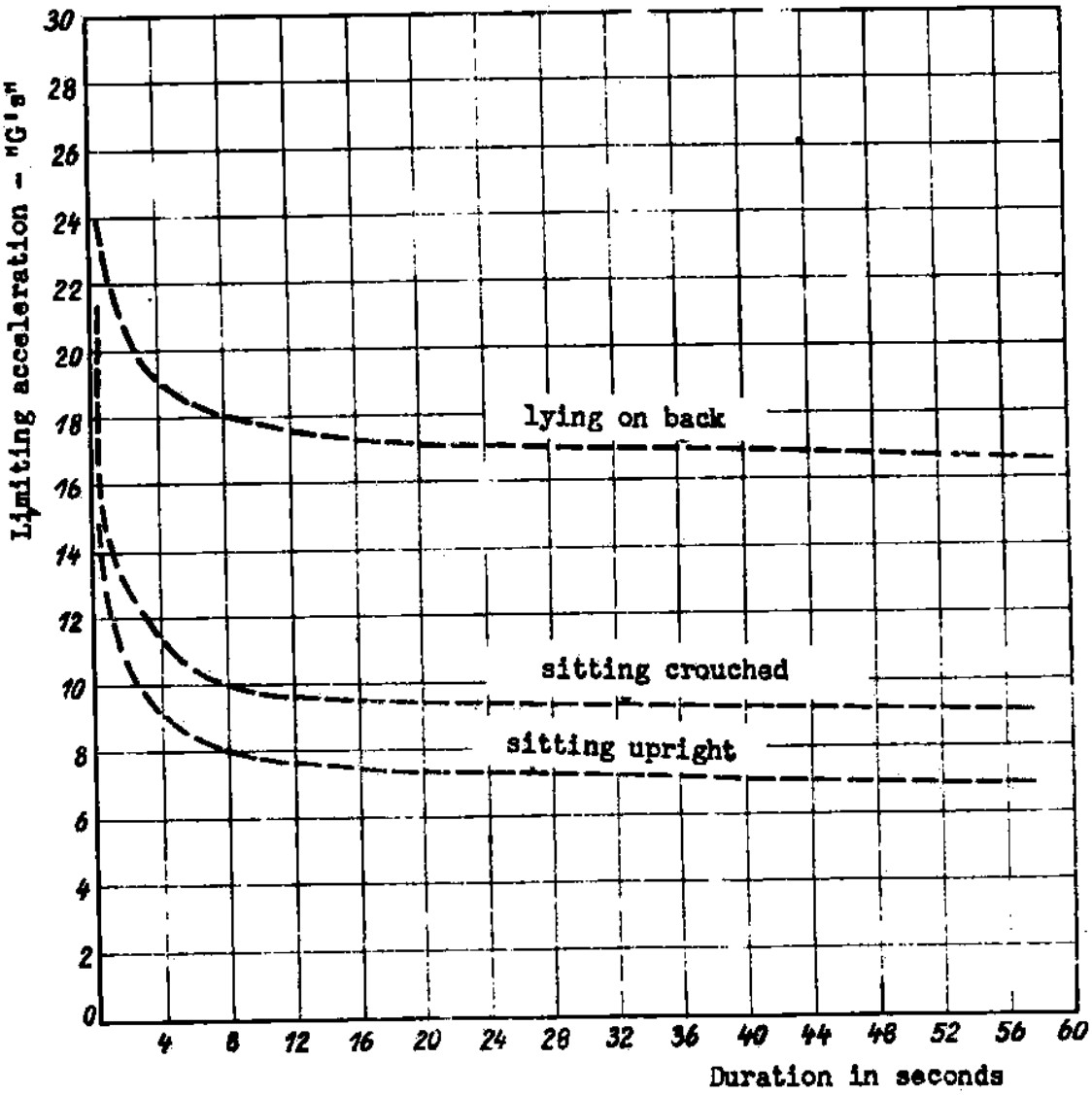

Fig. 53;

Limits of accelerations withstood by trained pilots in terms of "G's" as a function of time of duration

bomber, because of its long range and the accurate navigation necessary for the bomb release, cannot do without a pilot on board. Thus the permissible accelerations are limited to values that can be withstood by trained flyers.

In Fig. 53 are shown the results of most recent studies (2, 12, 15, 31) on the highest accelerations that are bearable by a man in different body positions, as a function of the length of the acceleration time. Whereas in the sitting position the limit is determined by disturbanc of the circulatory system especially caused by loss of blood from the brain or heart due to differences in hydrostatic level inside the circulatory system, this danger decreases in the lying position, and the limit then seems to be set by difficulties in breathing as a result of greatly increased weight of the thorax. This more favorable lying position is directly achieved in the seating arrangement sketched in Fig. 33, since the accelerations due to the engine are taken up by the pilot in directions perpendicular to the axis of his body. In the lying position in caroussel tests accelerations of 20 g for more than a minute have been withstood by drugged apes, and accelerations of 17 g for more than 180 sec. by men.

During the takeoff and climb of a rocket bomber there are two phases during which the accelerations can reach critical values: the catapult takeoff and the end of the climbing path. The catapult process at takeoff lasts several seconds; the accelerations can be chosen freely, the acceleration starts rather suddenly, keeps its top value for about 11 sec. and then stops again suddenly. Adjustment of the circulatory system is thus scarcely possible. Because of this impulse and rather long action, one cannot go beyond an acceleration at takeoff of more than 5 g, even for the favorable perpendicular position. Also higher takeoff accelerations, though they result in economizing on starting-rockets by decreasing the run on the ground, are unfavorable as regards flight performance, since they necessitate stronger construction of the tank assembly. Conditions are quite different at the end of the climb. During the climb the accelerations increase in the ratio G_o/G as the result of decreasing mass of the aircraft for constant motor thrust. Even if the aircraft flies without payload, this ratio will end up at 10. This climbing process lasts several minutes, with the greatest acceleration occuring in the last second. The body has plenty of time to adjust itself to the high accelerations, and the highest accelerations last for only a short time. The conditions are thus very favorable, and the effect of the high acceleration on flight performance is also favorable. One can, therefore, go closer to the limits of resistance and, in view of the perpendicular position of the pilot, permit accelerations of 10 g.

For the assumed $G/G_o = 1$, this means that the factor a equals 1, i.e., the motor thrust equals the initial weight. The limiting acceleration of 10 g is of course not reached if the bomber varries cargo. E.g., if it has only 5 tons of bombs on board, then $G/G_o = 0.15$ and the limiting acceleration is 6.67 g. For $P = G_o$, the acceleration at the start of the climb is 1 g, and increases in say $t = c/g \times (1 - G/G_o) = 340$ or 360 sec. to 6.67 g or 10 g respectively if we use the relation $b = g/(1-gt/c)$ which neglects frictional forces. The last increase from 6.67 g to 10 g thus occurs in the very short time of 20 seconds. Only during these last 20 sec. is the pilot subjected to the critical accelerations, after he has become accustomed to the high acceleration gradually and uniformly during the previous 340 sec.; furthermore, this holds only for the practically unimportant case where he takes off without bombs. With this the assumptions concerning permissible accelerations during climb seem justified.

2. Catapult Takeoff

The rocket bomber is to be brought to a takeoff speed of 500 m/sec by means of equipment on the ground, in order to increase as much as possible the final velocity attainable with the fuel on board, to minimize the difficulties associated with the initial wing loading of 800 kg/m^2, and to eliminate the uncertain flight characteristics of the airframe in passing the velocity of sound. For this purpose a catapult-like, perfectly straight, horizontal starting-track several kilometers in length is needed; on this sits a sled, which carries the aircraft, and which is driven by rocket apparatus having a large thrust but moderate exhaust speed. Fig. 54 shows a schematic of the sling arrangement. The downward forces acting along the takeoff path are the weight of the bomber with sled and starting rockets, about 150 tons; in addition there are large forces acting vertically upwards or in the direction of the path due to driving and retarding actions respectively. These forces and the necessity for very precise installation of the slide-rails suggest the construction of the roadbed out of reinforced concrete, whose cross-section for the single-track arrangement chosen has the isosceles triangle shape shown in Fig. 54; the base of the triangle serves to fix the structure in the ground, while the sled carrying the aircraft rides on the apex of the triangle. The upper construction of the rail arrangement consists of the main rail lying on top of the wall, which has to take up the perpendicular forces and also transmits the very large horizontal retarding forces, and of two lead-rails halfway up the wall, which support only occasional small forces, and which prevent rotations of the whole system of aircraft plus sled around its longitudinal axis. Lubricants of the proper viscosity are used on the main-

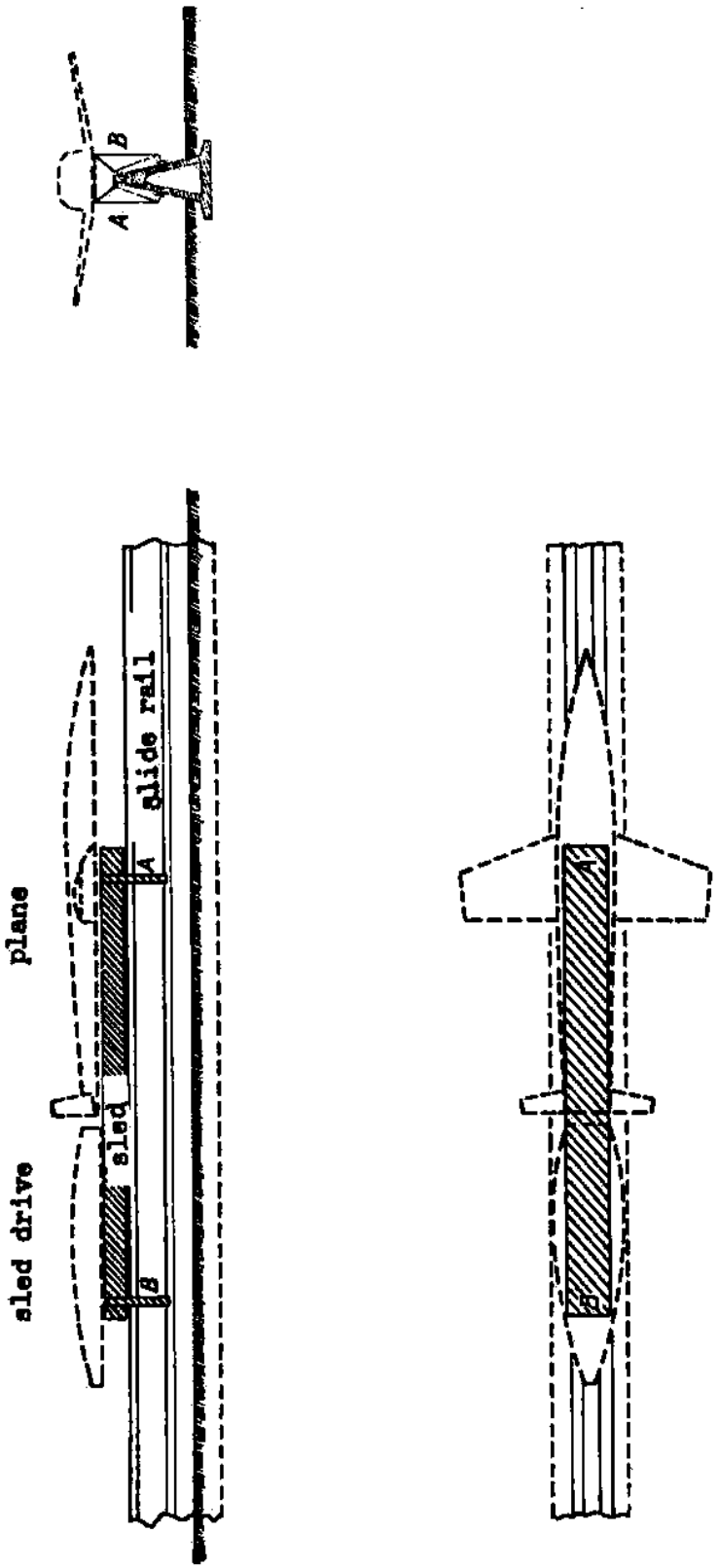

Fig. 54; Starting sled of the Rocket Bombers

and lead- rails, so that the sliding faces of the sled can glide on them with little friction. The sled itself is mounted on the sliding faces at A and B and also has a pair of fittings to prevent overturning. The aircraft to be catapulted sits up front on the main body of the sled, the sled's power plant is at the back, behind the aircraft. The high takeoff thrusts are transmitted to the aircraft through the main body of the sled. Very high thrusts of 610 tons for 11 seconds and the utmost safety in operation are required of the starting rockets, while their exhaust speed can be moderate since they do not affect the flight performance of the bomber. In the use of 40 tons of fuel for starting, one will not, for reasons of safety and cost, use the selfacting fuels like powder or H_2O_2, which are customary for moderate exhaust speeds, but rather the fuels consisting of two materials, say liquid O_2 and gasoil-water emulsion, are preferable. For the calculation of the catapult process, we shall take, as exhaust speed of the ground-based starting rockets, C = 1500 m/sec. so that the fuel consumption per second is Pg/c = 4000 kg/sec. The weight of the whole apparatus, for constant starting thrust P, is $G_s = G_{os} - Pgt/c$ at any instant. The air resistance of the whole catapult system is estimated to be 75,000 kg for $\frac{V}{a} = 1.5$, and increases during the takeoff according to the equation $W = 0.3\ V^2$. The sliding friction of the sled on the takeoff rail is completely negligible compared to the two forces mentioned. Using the second law of motion we can write for the acceleration at any moment during takeoff: $dv/dt = g(P - 0.3v^2)/(G_{os} - Pgt/c)$

If we require that the acceleration at the end of the takeoff shall not exceed 50 m/sec^2, then we obtain for the constant starting thrust P value of 610,000 kg if the final weight of the take-off mass is 105,000 kg. By integrating once, we obtain a relation between time elapsed and velocity attained $t = G_{os}/3990.\left[1 - \left(\frac{428 - 0.3v}{428 + 0.3v}\right)^{2.48}\right]$

For V = 500 m/sec we obtain for the time of takeoff $t_1 = 7.37 \times 10^{-5} G_{os}$; the law of consumption of the takeoff rocket yields a second relation: $G_s = 105000 = G_{os} - Pgt_1/c$ from which t_1 = 10.96 sec and G_{os} = 148700 kg. The total path length can be obtained most simply by numerical integration. Summarizing, these relations concerning the takeoff process give the results that: the takeoff rockets develop a thrust P = 610 tons for 11 sec, use up 43.7 tons of fuel with c = 1500 m/sec if the system to be catapulted weighs 105 tons, the length of the tow path is 2750 m; and that the accelerations during towing increase from an initial value of 40.2 m/sec^2 to the permissible limit of 50 m/sec^2 at the end of the takeoff; thus for approximate estimates one may use an average acceleration b = 45 m/sec^2 and calculate all the other quantities; e.g. $t = v/b = \frac{500}{45} \doteq 11\,\text{sec}$ and $s = \frac{1}{2}bt^2 \doteq 2750\,\text{m}$.

Fig. 55 shows the dependence on length of path of the velocity V attained and the residual weight G; also given are some of the data concerning the sliding jaws of the takeoff-sled. The two sliding jaws at A and B can be assumed to be of bronze or hard steel and have a square jaw-surface of 0.25 x 0.25 m; they are a sort of self-adjusting bearing-plate in Michell bearings, and are movable about a hinged edge; the flat undersurface of the jaw is bent up at the front end to assure the flow of lubricant to the edge. From Gumbel - Everling (7, P. 150/151) one obtains, for a square sliding jaw of side length t, if the point of application of the force corresponds to the safest thickness of lubricating layer ($\chi_1 = 0.8$), some fundamental equations; e.g., the coefficient of friction is $\mu = 2.37\sqrt{\eta v/pt}$, where p is the average pressure P/t^2 on the jaw; the minimum thickness of lubricating layer is $h_o = 0.30t\sqrt{\eta v/pt}$, and the angle of tilt is $\alpha = 0.37\sqrt{\eta/pt}$.

From these, $\mu = 7.97 h_o/t$ i.e., the minimum gap h_o between the sliding jaw and the rail surface, which make an angle α with each other, should be kept as small as possible to permit large loads P to slide with little frictional resistance. In the desired state of pure liquid friction, h_o is limited by the roughness of the sliding surfaces; for the long sliding surfaces of the takeoff track which is subject to rough handling and all kinds of weather, we may expect values of 10^{-4}-10^{-5} m. Thus the minimum gap-height h_o to assure dynamical buoyancy of the jaws is $h_o = 10^{-4}$ m, with $\mu = 0.00316$. The largest section-loading ever experienced by the jaws is $p = 75000/625 = 120$ kg/cm^2; during takeoff this drops to 4 kg/cm^2. From the previous equations we see that minimum thickness h_o (and the minimum μ) can always be maintained, if the viscosity η of the lubricant, decreases in the same manner as V/p increases; i.e., if $\eta v/p$ is constant. At the start of the motion of the sled, the sliding speeds are so small that there is no η sufficiently large to keep the product constant. In this case, the flat surface of the jaw will lie flat on the surface of the rail and will rise to the angle α only as the velocity increases. Fig. 55 shows the residual part G-A of the weight G which rests on the jaws at any moment; it is assumed that the buoyance A varies quadratically with V from A = 0 for V = 0 to A = 100 tons for V = 500 m/sec. Thus $P = \frac{G-A}{2}$ and the required lubricant viscosity at any position on the track is $\eta' \doteq 11.1\,Ph_o^2/vt^3$. η' is the viscosity of the hot oil in the film for minimum thickness h_o. The rise in temperature ΔT of the oil film can be estimated by assuming that all the work against friction goes to heat the oil. Because of the very brief duration of this heating process, the heat conduction from the oil will be extremely small. From $APfv = th_o v\gamma c_s \Delta T$ it follows that the heating is independent of the velocity; taking values of

$\gamma = 900\ \text{kg/m}^3$, $c_s = 0.5\ \text{kcal/kg}^\circ$, ΔT is $0.000834\,P$

so that as P decreases it drops from 60° to about 2° C at the end of the catapult process, as shown in Fig. 55. If we assume an external temperature of + 15° C, then at the end of the tow path a lubricant is required which has a viscosity of $\eta = 0.00002$ at +17° C; e.g., benzine, water, petroleum; three meters from the beginning of the takeoff we need a lubricant with $\eta = 0.1$ at 75° C; this requirement is satisfied by pitch. In between there is a whole range of possible lubricants. In the first three meters of the slide, pure liquid lubrication will not be possible; one will have to use graphite-pitch mixtures. The equations given are valid only for moderate sliding speeds; actually the velocity of motion reaches a final value of 500 m/sec which is 1/3 the velocity of sound in the lubricant; because of this we may expect a great increase in the coefficient of friction, but no physically different friction phenomena, especially since the high velocities are accompanied by small pressure on the sliding jaws. The proper lubrication of the 3 km long surface should be maintained and protected by a special lubricant carriage which runs the full length of the track, along the rails. The brake arrangement at point B can be modelled on that of a railroad; i.e., cast-iron jaws are pressed onto the braking surfaces of the rail; after the aircraft rises the forces are released and the empty sled is brought back to rest as quickly as possible.

To test the basic feasibility of sliding at high speeds, R.Schmid has made tests on the sliding of projectiles along curved metal walls lubricated with vaseline. The experimental arrangement consisted of a drawn-steel tube of 10 mm inner diameter, which was slit along its axis to produce a U-shaped groove. This channel was bent into a closed circle 8 m. in radius, so that the surface of the channel was toward the outside; then the projectile sliding in the channel is kept there by centrifugal force. Through a branch tube which was tangent to this circle, an sS projectile was fired from a German 98 K, and into the circular path. The bullet ran through the circular path several times till it was brought to rest; after the test it was found lying completely unharmed in the channel (Figs. 56, 57, 58)*. The thin copper plating of the steel was, in most tests, rubbed off at the position of the maximum diameter; the steel surface showed isolated scratches apparently caused by filings and burrs along the slide-path. Immediately after finding it, the bullet was still warm to the touch. Also it was compressed in cross-section; this is probably caused by the fact that the spinning of the bullet stops after a short time and then the centrifugal force, which is initially 100 kg, causes the lead core to flow. After cessation of rotation and slight deformation, the initial point contact with the wall is increased to a surface of about 1 cm^2, so that the 100 kg/cm^2 pressure between the surfaces, which is caused by the centrifugal force, corresponds approximately to that of the sliding jaws of the takeoff sled. Since the sS -bullet is made of lead with a thin soft steel cover, and in the course of its 150 m. sliding path goes through all velocities from 800 m/sec down to zero without being harmed, this experiment may be considered as a proof of the feasibility of construction of sliding jaws for velocities of 500 m/sec; provided the slide-rails are properly constructed and lubricated.

If the accelerations of the aircraft during its launching are to remain within permissible limits for both aircraft and pilot, a launching path of about 3 km. is required, so that it is not possible to use a movable construction which would point the craft toward its target at takeoff. One will therefore install a takeoff track, usable in both directions, so that it points in the most probable directions for attack, say east-to-west; the more precise correction of the direction of flight can be left to the pilot during the very first part of the climb path, where the velocity and acceleration are still sufficiently small to permit such changes of path.

If the bomber rises off the takeoff-sled at 500 m/sec, then its lift coefficient is $c_a = 0.05$, whereas the best glide-number occurs at much larger angles of attack and a lift coefficient $c_a = 0.173$. If one limits the normal acceleration during the first driveless part of the climb-path to 20 m/sec^2, then the initial radius of the turning-path, which goes from the horizontal takeoff direction to the direction of climb at $\varphi = 30°$, is 12500 m. This curved path of turn, which begins at the end of the takeoff is 6540 m. long and ends at an altitude of 1700 m., with the required path inclination of 30° As a result of air resistance and gain in altitude, the velocity at this point has dropped to 370 m/sec, the lift coefficient is $c_a = 0.093$ - still much smaller than the one for optimum glide-number. The bomber then climbs further at an angle of 30°, at the expense of its flying speed until, after a linear climb of 4000 m. to a height of 3675 m. and a velocity V = 284 m/sec, the angle of attack for optimum glide-number is reached; at this moment the rocket drive for the actual climb can begin. During this 25-second-long, undriven motion after takeoff, the path of the aircraft can be turned in the direction of the target. At the same time, this procedure helps increase the range of the bomber over its value if one took off at V = 250 m/sec with optimum glide-number and started the engine immediately after takeoff, because we have gained a slight excess velocity and a few kilometers for the climb.

*These Figs. omitted

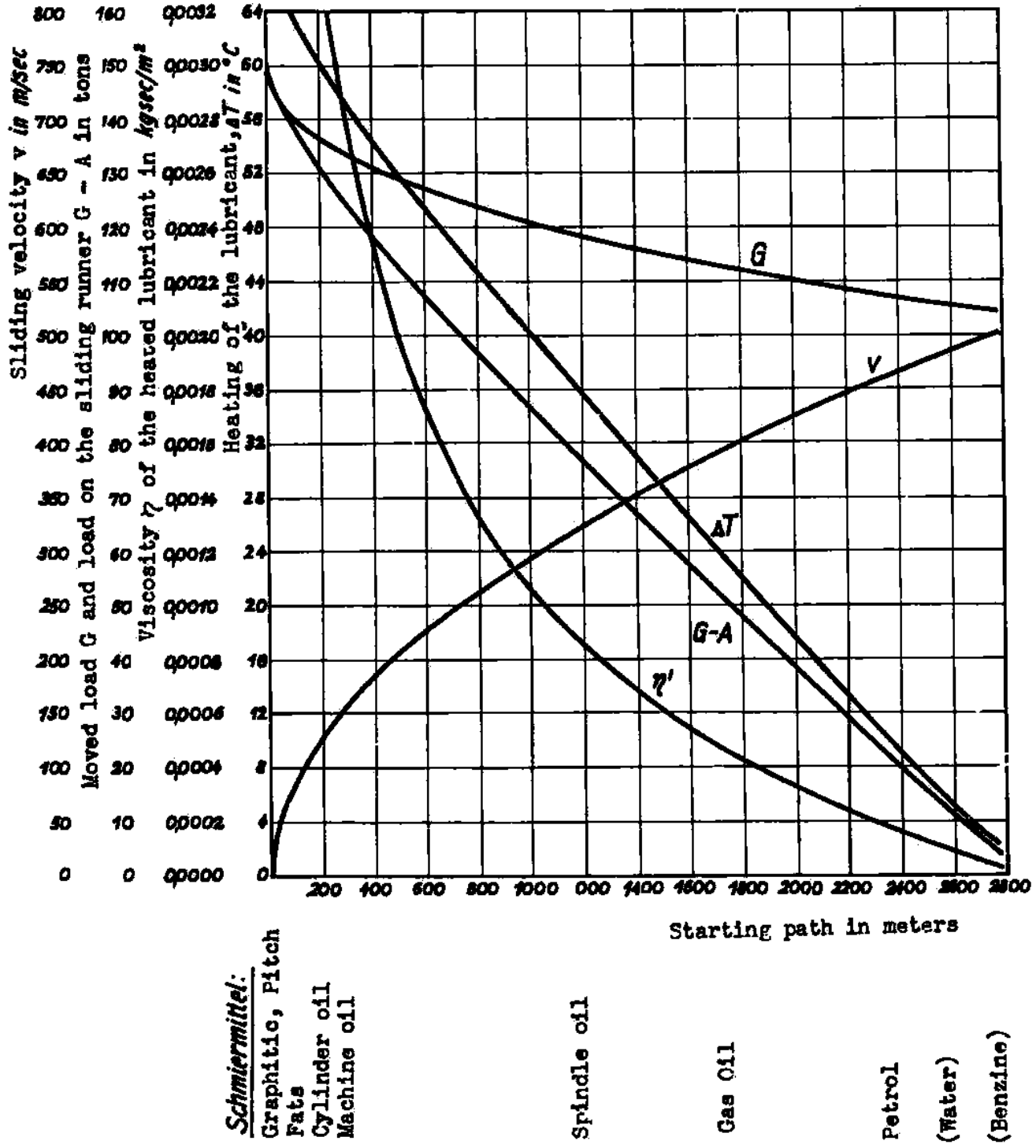

Fig. 55; Gliding velocity v, moved load G, loading on the runners G - A, heating of the lubricating film ΔT, viscosity η of the heated lubricating agent, and practical manner of lubricating for various points along the starting path.

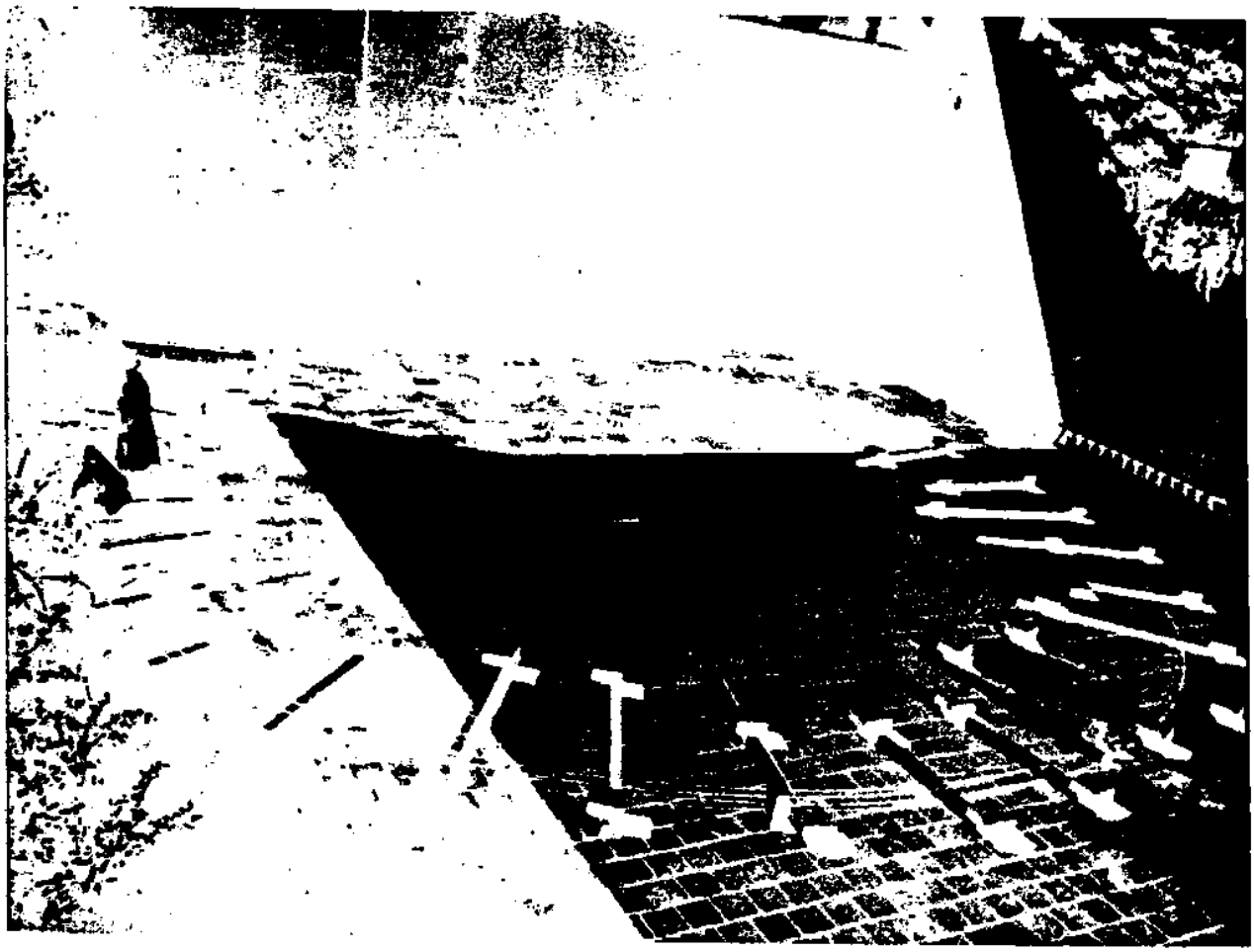

Abb. 56; Versuchanlage für Gleitreibungsversuche bei sehr hohen Gleitgeschwindigkeiten, bestehend aus einem Militärkarabiner 98K und einer mit 5 m Radius gekrummten, geschmierten und geschlossen-kreisformigen Gleitbahn für das sS-Geschoss.

3. Climb Path

The climb path of the rocket bomber is determined by the forces acting on its center mass. If one momentarily neglects the rotation of the earth, these are:

The weight of the aircraft-magnitude $G = (G_0 - P_g t/c)[R/(R+H)]^2$ direction toward the center of the earth.

The aerodynamic lift-magnitude $A = c_a F \rho v^2/2$, direction perpendicular to the tangent to the path and in a plane through the center of the earth;

The air resistance-magnitude $W = \varepsilon A$ in the direction of the tangent to the path;

The thrust of the motor-magnitude P = 100 tons, tilted from the tangent to the path by angle of attack, lying in the plane through the center of the earth and the tangent to the path.

The d'Alembertian inertial force T, equal and opposite to the resultant of the other forces, having a tangential component $m\frac{dv}{dt}$ and a normal component $m\ Va^2/\rho$.

These five forces all lie in a plane, so that the path is also in a plane.

The rotation of the earth makes the situation more complicated. If the earth's atmosphere were fixed in space, so that it did not rotate along with the earth, then the path relative to the earth's surface could be calculated as if a sixth force, the Coriolis force, having arbitrary direction and magnitude $C = 2[\vec{\omega} \cdot \vec{v}](G/g - F/c)$ acted on the center of mass of the aircraft. Because of its arbitrary direction in space, this force makes the orbit, relative to an observer on the earth, appear to be no longer in a plane. The atmosphere, which actually rotates with the earth, produces dragging forces on the bomber which cause its absolute path also to be twisted, so that the bomber is pulled like a weather vane by the apparent wind developed by the rotation of the atmosphere, and will tend to turn except when it is flying in the west-east direction, as can be seen by considering a flight starting from the pole. This interfering weathervane action will have to be countered by the pilot's steering; i.e., by a seventh force perpendicular to the tangent, if the absolute path prescribed by celestial navigation is to be maintained. In the calculation, it is assumed that the transverse aerodynamic forces excited by the elimination of the weather-vane action do not noticeably alter the glide-number. Since these transverse forces are always perpendicular to the plane of the orbit and only prevent a shift of the aircraft out of the plane, they need no longer be considered in the calculation of the orbit. To illustrate the the relation between the forces acting on the center of mass, Fig. 59 shows two views of the aircraft during the climb; the line of sight is along the horizon at the level of the aircraft. If all the dependences were available in analytic form, one could introduce suitable space coordinates, resolve the forces along these directions, apply the dynamical equation to each direction and thus obtain three differential equations for the three coordinates of the climb path; the integration would almost certainly be impossible, since the far simpler equations of ordinary exterior ballistics are not. The determination of the relative orbit is much simpler; one proceeds in two steps; first the absolute path is calculated neglecting the Coriolis force (i.e., using the five forces previously listed). Then one calculates separately the turning of the earth's surface below the aircraft. Finally, the two components are combined on the sphere to give the twisted relative path in space. The plane absolute orbit is determined by a step-by-step method which is familiar in Ballistics. (1, Vol. 1, p. 207) As in Fig. 60, the continuously curved path is broken up into a polygon, whose sides are sufficiently short that they can replace the arc of which they are the chord. All the forces acting on the aircraft are combined at the vertices, A, B, C, etc., and along with the inclination φ of the orbit are assumed constant along $\Delta s = \overline{AB}, \overline{BC}$, etc. By setting the resultant force in the tangential direction equal to zero, we obtain $b_1 = g(P\cos\alpha - \varepsilon A_A - G_A \sin\varphi_A)/G_A$

so that the velocity increases in first approximation from V_A to $V_{B1} = \sqrt{V_A^2 + 2b_1 \Delta s}$ in the time $\Delta t_1 = V_B - V_A/b_1$. By setting the resultant normal force equal to zero we obtain $\rho_{A1} = G_A V_{A1}^2/(G_A \cos\varphi_A - P\sin\alpha - A_A)g$. The absolute velocity Va_A at the point A can be determined with sufficient accuracy from the velocity of flight V_A and the angular velocity of the point of takeoff. Thus the arc $\overset{\frown}{AB}$ can be drawn, and B, is determined in first approximation. Now that the average value of the inclination and the average force between A and B, are known, one can locate B in second approximation in the same manner. One repeats the procedure at B, often enough so that the orbit is given in analytical or graphical form. The calculations of the orbit by this method were done numerically by A Woyczechowski; the initial conditions were height 3675 m. above sea level, relative velocity of flight 284 m/sec, and inclination of orbit 30°, and the path was studied out to $G/G_0 = 0.1$. The orbit was also calculated for $c = 3000, 4000$ and 5000 m/sec and finally neglecting the earth's rotation, and then with maximum effect of the

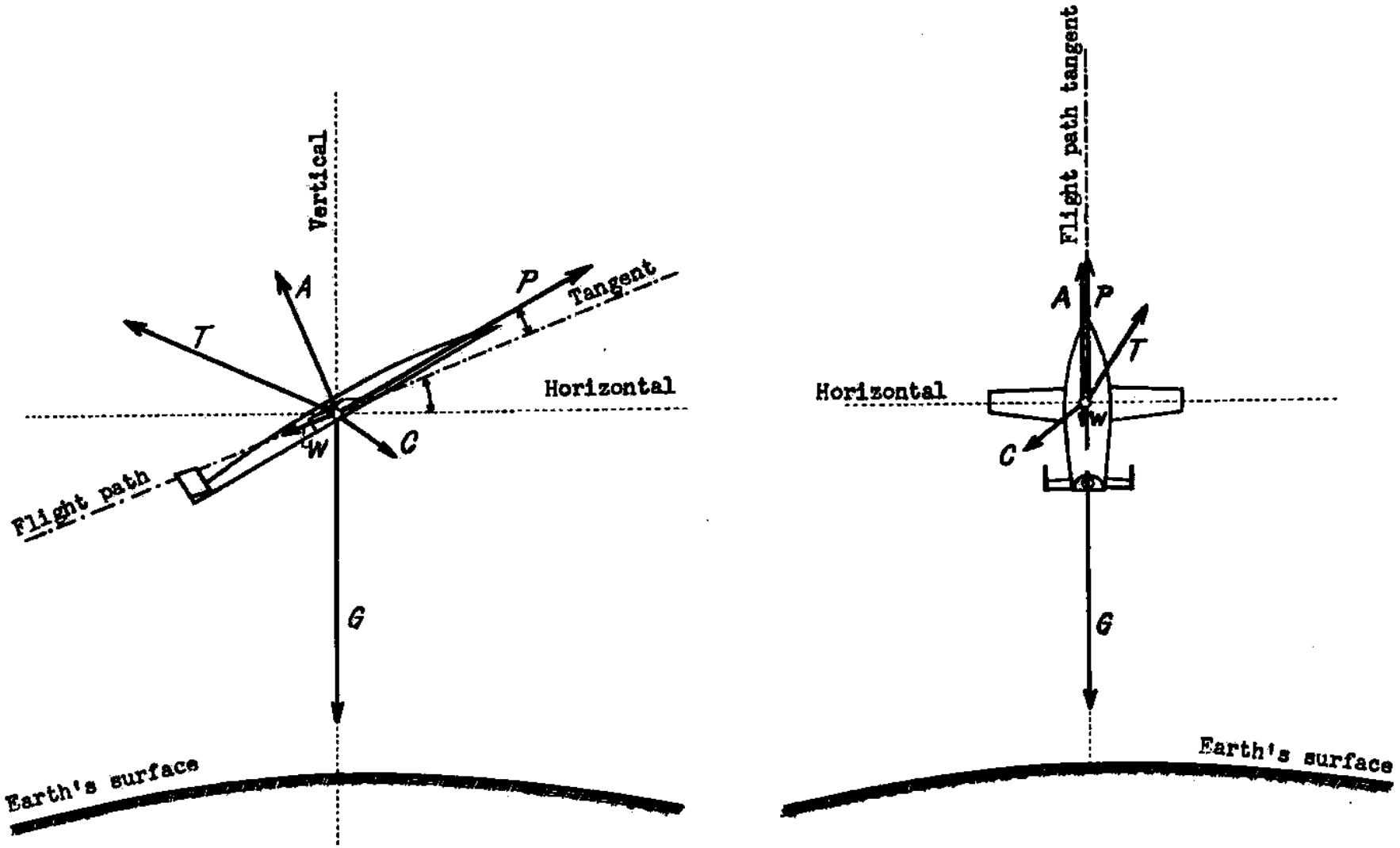

Fig. 59; External forces on the Rocket Bomber in climbing.

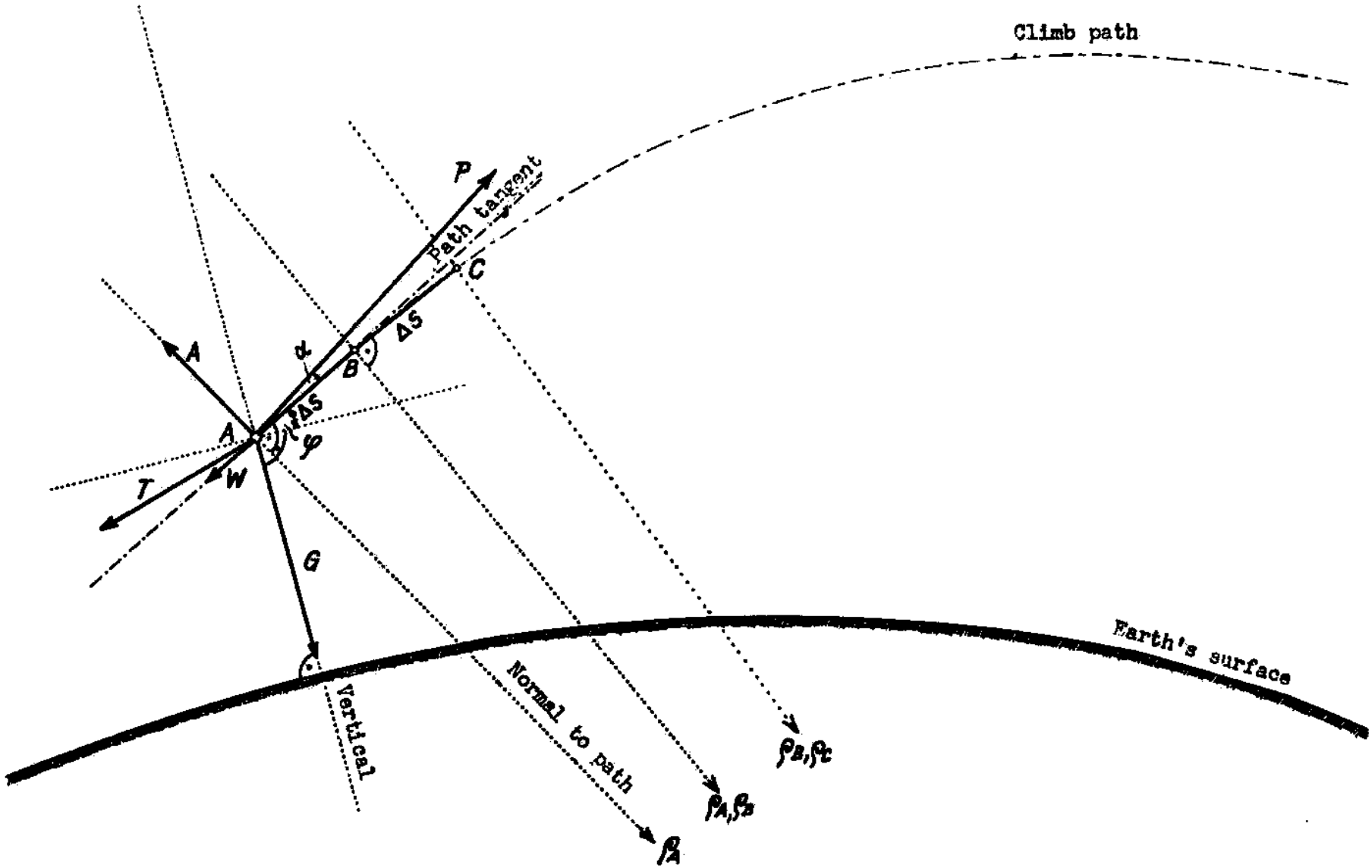

Fig. 60; Approximate graphical solution for the climb path

Exhaust velocity in m/sec	Flight Velocity v in m/sec	Instantaneous wt / Initial wt.	Bomb load in tons	Altitude in Km	Horizontal projection of the climb path in Km	Angle in degrees between horizon and the terminal tangent	Axial acceleration in m/sec^2	Normal acceleration in m/sec^2	Elapsed time in seconds
c-3000 m/sec	1000	0,60	50,0	37,0	55	+15,5	12,8	-6,8	124
	2000	0,42	31,8	46,5	135	+ 0,4	22,0	-6,7	178
	3000	0,30	20,0	41,5	230	- 4,1	30,4	-4,8	214
	4000	0,22	11,5	36	320	- 3,7	41,0	+3,7	240
	5000	0,15	4,8	34,5	405	+ 1,2	55,8	+37,0	261
	6000	0,10	0,3	40	485	+ 7,3	77,3	+39,1	274
c-4000 m/sec	1000	0,69	58,7	33,5	60	+ 8,2	12,1	- 7,1	124
	2000	0,53	43,3	31	150	- 8,1	19,1	-5,5	189
	3000	0,40	30,5	44,5	280	+7,6	18,3	+ 26,8	243
	4000	0,30	20,0	47	425	+9,5	28,3	- 2,4	283
	5000	0,23	13,3	68,5	560	+8,1	37,7	- 4,0	313
	6000	0,18	8,0	84	675	+7,4	47,5	- 3,0	333
	7000	0,14	3,8	98,2	785	+7,3	61,3	- 0,8	350
	8000	0,11	1,0	109	860	+7,6	81,6	+ 1,6	362
c-5000 m/sec	1000	0,75	65,0	31	60	+3,1	11,5	-7,3	128
	2000	0,62	51,7	18,5	155	-10,6	16,3	+5,0	196
	3000	0,48	37,5	43,5	335	+11,9	16,7	-3,9	267
	4000	0,38	28,1	71	505	+7,3	22,3	-6,3	315
	5000	0,30	20,1	87,5	665	+4,4	28,8	-5,8	351
	6000	0,25	15,0	98,5	830	+2,9	34,8	-5,1	380
	7000	0,20	10,5	106	975	+2,6	41,0	-4,1	404
	8000	0,17	6,5	112,3	1135	+1,8	49,5	-2,9	424
	9000	0,14	3,5	117	1275	+2,0	60,3	-1,3	440
	10000	0,11	1,0	121,5	1400	+2,3	73,3	0,4	452

Numerical characteristics for three various climbing paths of the Rocket Bomber.

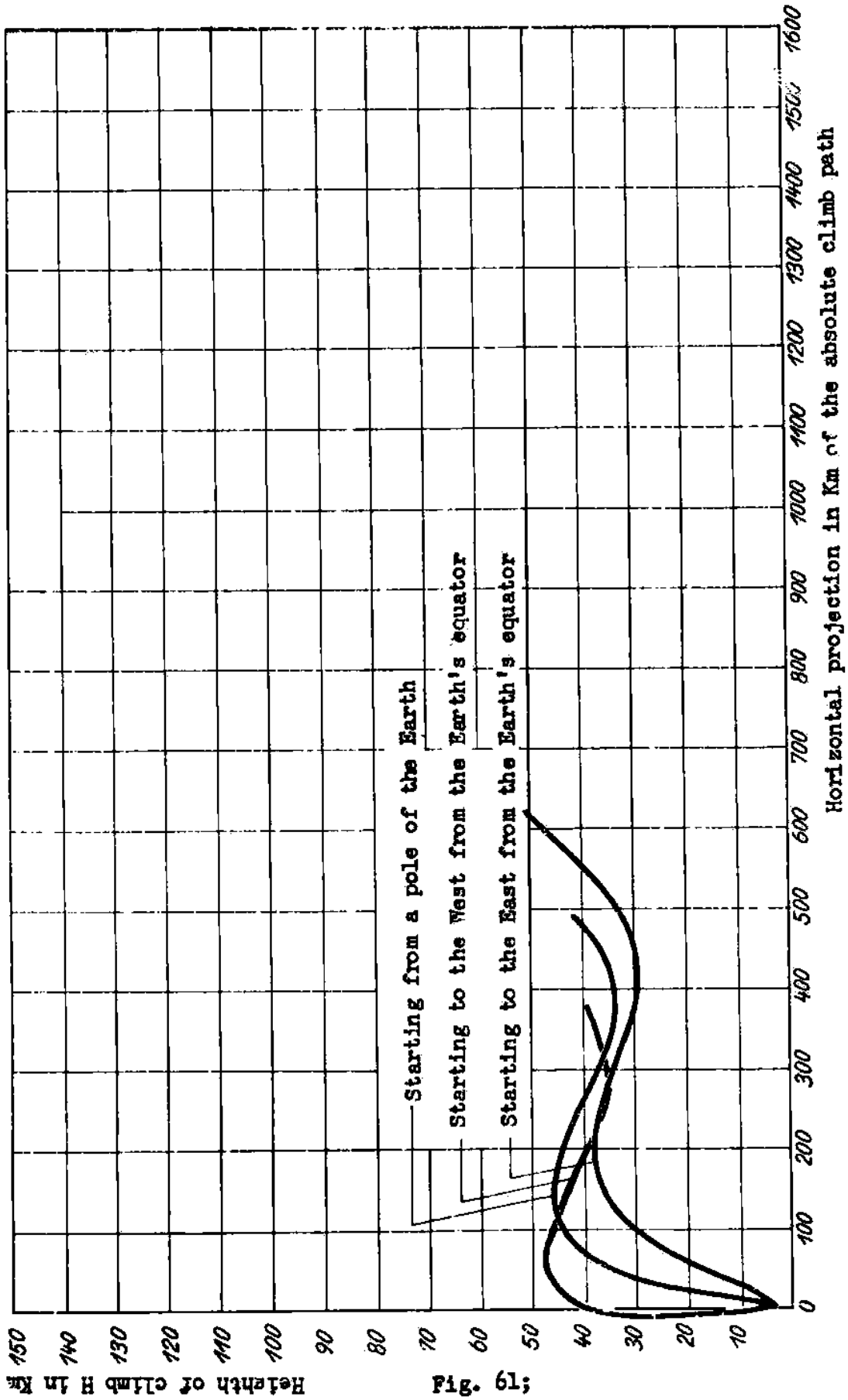

Fig. 61;

Absolute climbing path of the Rocket Bomber with c = 3000 m/sec, without consideration of the Earth's rotation, but with consideration of rotation velocity of a point on Earth's equator, launch to East and launch to West.

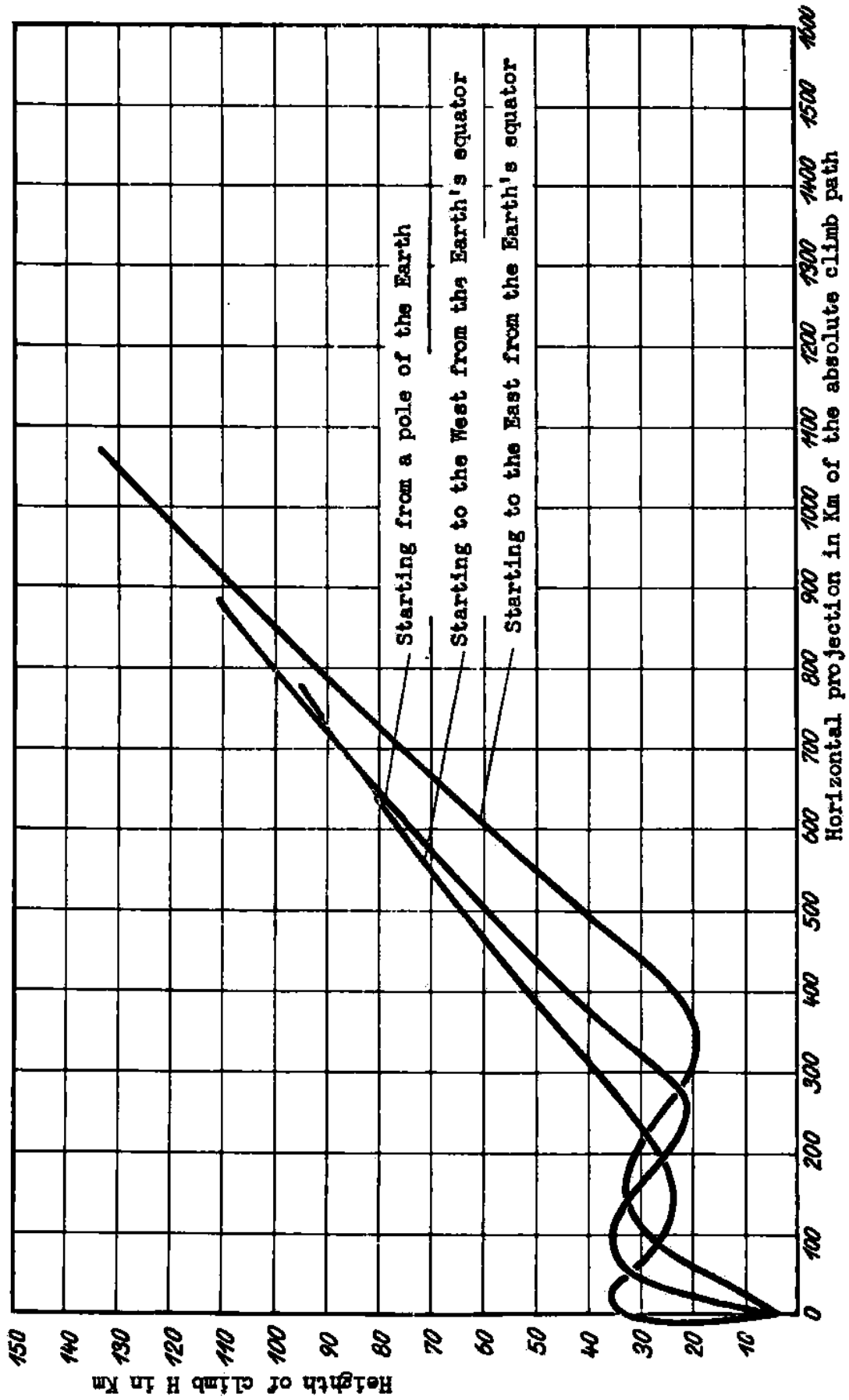

Fig. 62: Absolute climbing path of the Rocket Bomber with c = 4000 m/sec, without consideration of the Earth's rotation, but with consideration of rotation velocity, of a point on Earth's equator, launch to East and launch to West.

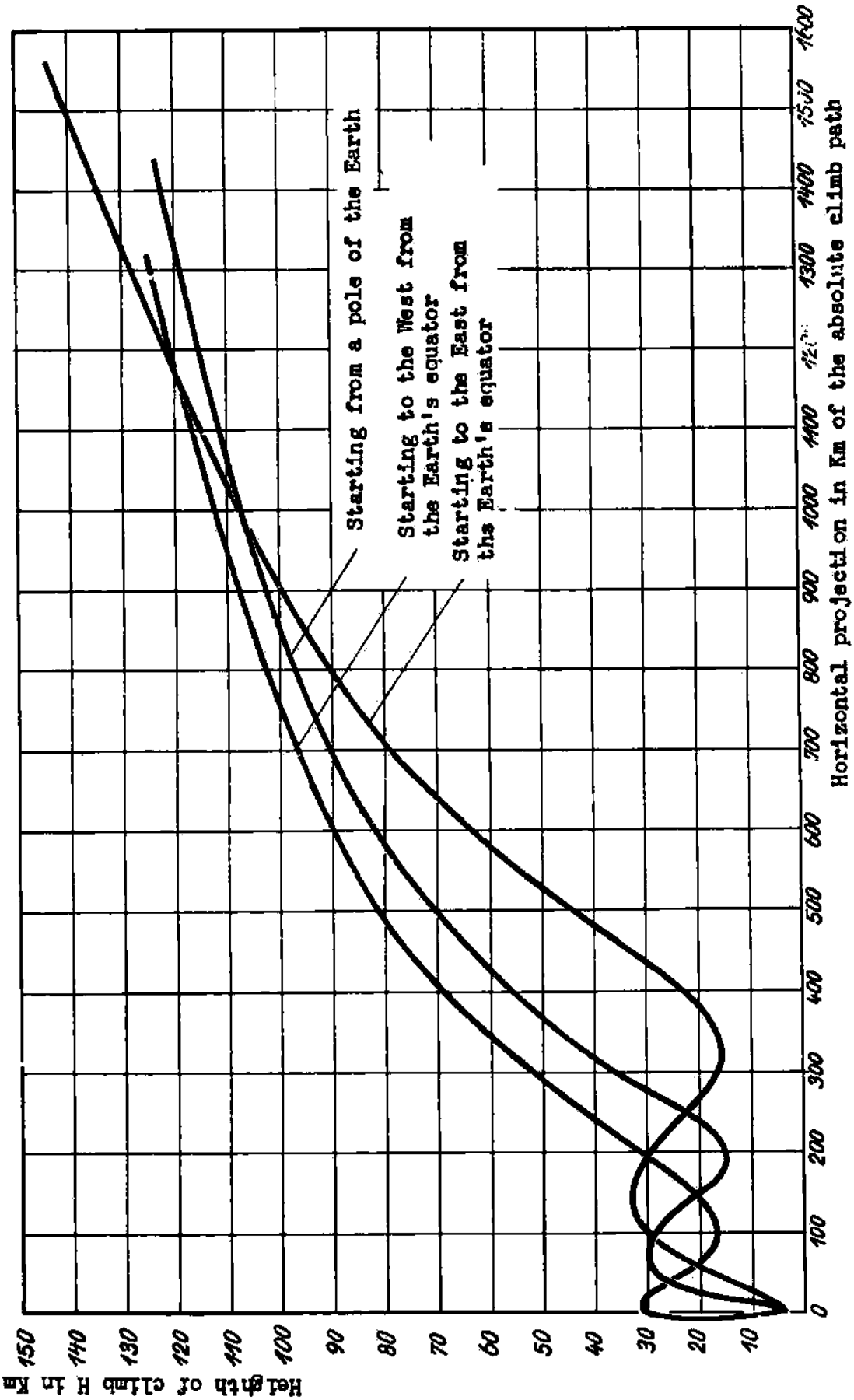

Fig. 63: Absolute climbing path of the Rocket Bomber with c = 5000 m/sec, without consideration of the Earth's rotation, but with consideration of rotation velocity, of a point on Earth's equator, launch to East and launch to West.

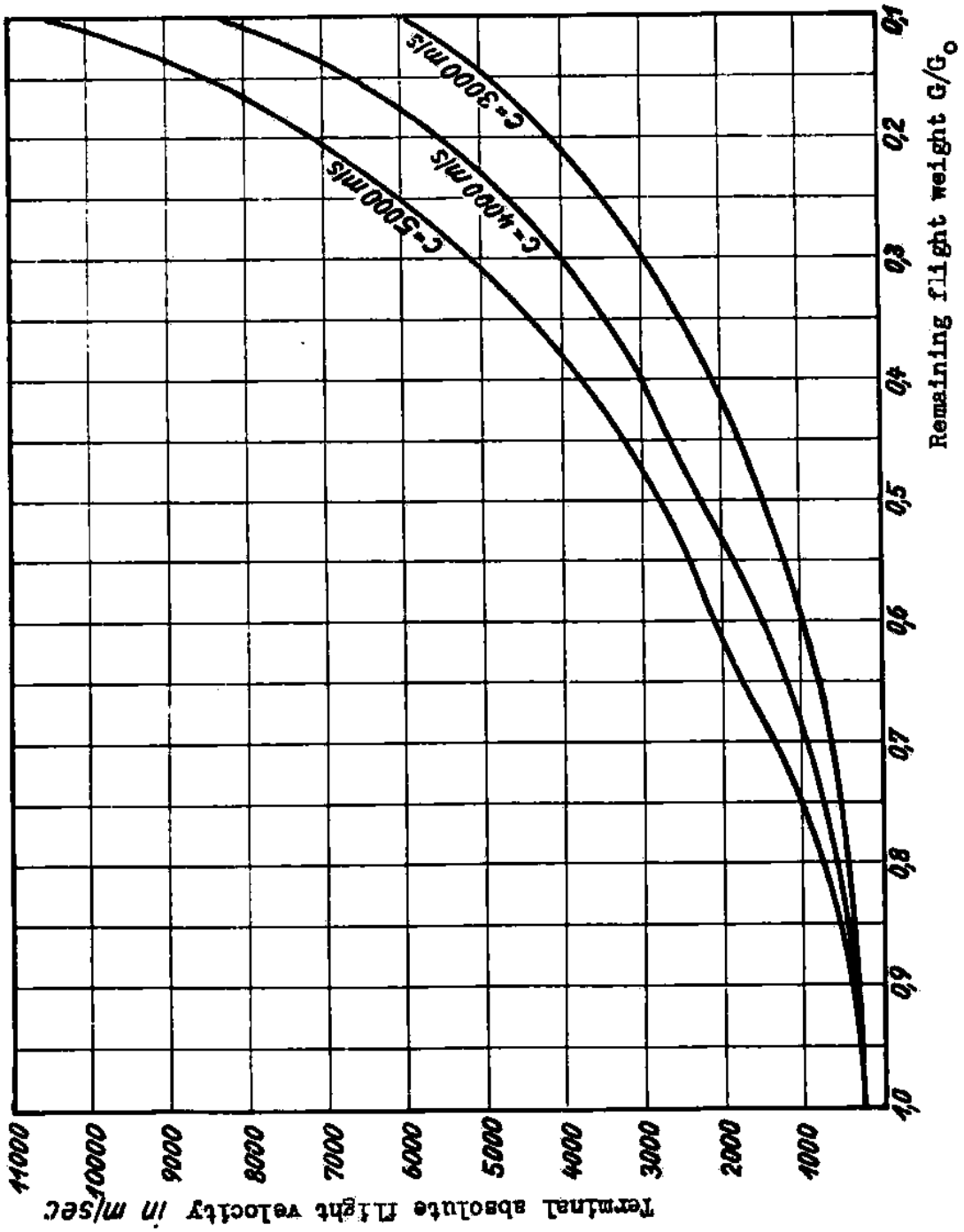

Fig. 61: The absolute flight velocity of the Rocket Bomber attained during climb with c = 3000, 4000, and 5000 m/sec as a function of G/G_o, and without consideration of Earth's rotation.

rotation - i.e., takeoff from the equator in an easterly or westerly direction. The following figures show some examples of the results; Fig. 61-63 show the shape of the absolute orbit, Fig. 64 shows the velocities reached. Table III gives a summary of the most important results for all the orbits, neglecting the earth's rotation.

A fairly accurate estimate of the final velocity, which is the most important datum for the climb path, can be obtained without doing the exact calculation of the orbit, by using the equation $V/c = \ln G_o/G - q(1 - G/G_o)$ This is especially so if one fits the actual conditions by setting q (ratio of total air resistance plus weight component along the path to instantaneous weight) equal to 0.5 in the range $G/G_o = 1.0$ to 0.5, and q = 0 for $G/G_o = 0.5$ to 0.1. If one carries out this rough calculation for the bomber with 100 ton takeoff-weight and 10 tons empt, weight, for various exhaust speeds C, assuming initial velocity 284 m/sec, one finds that for C = 4000 m/sec the bomber reaches the velocity of a long-range projectile even with a 50-ton bomb load, so that it can compete with long-range artillery; without payload it exceeds the velocity V = 7900 m/sec. Between these two extremes lie all sorts of velocities and bomb loads. An interesting result which is easily obtained, is that in the range of bomb loads suitable for military use, i.e. 5-40 tons, the exhaust speed has little effect on the final speed. This means that the development of a rocket bomber does not have to wait for availability of rocket motors with C = 4000 m/sec; with C = 3000 m/sec one can already construct a very dangerous weapon.

Figs. 65 and 66 compare this rough calculation to exact orbit calculation and to the curve for ideal rocket propulsion; the initial velocity after takeoff is included. One sees that the rough estimate gives the actual behavior with sufficient accuracy, especially for large values of C; also the final velocities actually attained, especially with large bomb loads, are far below those for ideal rocket propulsion, because the weight component in the direction of propulsion is comparable to the thrust for the initial steep climb, and because of the rather high air resistance during the climb. The propulsion curve could thus be improved by lessening the resistance or increasing the propulsive forces. A lowering of the initial angle of climb φ would decrease the harmful weight component, but would result in great increase in air resistance in regions of dense air - we can expect no success from this procedure. Another possibility might be a great increase in the thrust during the initial part of the path, so that, say, the tangential acceleration is constant in the range of the permissible limit 10 g, and the resisting forces are half the instantaneous weight initially and then drop to zero below $G/G_o = 0.5$. The rocket motor would have to start with a thrust of 1000 tons, and then be throttled gradually to 100 tons at the end of the climb. Taking $V = 284 + 0.95c \ln G_o/G$ for $1.0 > G/G_o > 0.5$ and $V = 284 + 0.659c + c \ln G_o/2G$ for $0.5 > G/G_o > 0.1$ we get the results shown in Fig. 67. While the 100-ton rocket motor weighs 2500 kg, one must assume a weight five times as great (i.e., 12500 kg) for a well-regulated motor with 10 times greater maximum thrust. If, despite the more powerful motor, all other weights of the bomber remain the same, then the empty weight would be 20000 kg. instead of 10000 kg; i.e., the most favorable G/G_o would be 0.2, and the bomb load would already have dropped to zero at $G_o/G = 5$. The propulsion curve shown in Fig. 67 for 10-ton empty weight would, for the now necessary 20-tons, move considerably to the right; despite the increased difficulties with the regulable 1000-ton motor one would achieve only a slight improvement for short distances of attack, while the 100-ton motor would still be superior for long range attacks. Thus the second method for improving the propulsion curve also fails in practice, and the curves of climb shown in Figs. 65 and 66 represent the best solution of the problem.

The rocket bomber, at each moment of its flight, tends toward that part of the atmosphere where the buoyant forces are equal to its weight. If this equilibrium position is such that the altitude stays constant for a few seconds, it will be said to be stationary. Such a stationary equilibrium occurs, for example, if the aerodynamic driving force A of the bomber, increased by the centrifugal force F, which for flight at constant altitude is a consequence of the earth's curvature, is equal to the instantaneous weight G of the bomber.

During the climb the thrust component $P\sin\alpha$ also acts as a buoyant force. For example, starting with a weight in flight, G_o = 100 tons, at altitude H_o = 3500 m, and C_{a_o} = 0.2, by equating the weight to the propulsive force, we can obtain for the horizontal velocity a value $V_o = \sqrt{2g G_o/c_{a_o}\delta F} = 300$ m/sec. At any other altitude, if we set the weight equal to the buoyant force $c_a \delta v^2 F/2g + Gv^2/gR = G$ we get a one-to-one relation between altitude and velocity. This relation is shown in Fig. 68, for C = 4000 m/sec. We see that these stationary altitudes are low, below 60 km for velocities up to 7000 m/sec. If we include the vertical component, $P\sin\alpha$ of the motor thrust of 13920 kg, we get the upper curve. It is interesting to note that for V = 4700 m/sec., the curve becomes vertical; i.e., no stationary equilibrium is possible at finite altitude as soon as V = 4700 m/sec. In the first curve the stationary equilibrium is no longer attainable above V=7900 m/sec. These assumed stationary states probably do not exist in flight. In particular, the center of curvature of the path is seldom at the center of the earth so that the altitude would remain constant - most of the time it is near the earth's surface, and at times it is even above the aircraft; also the radius of curvature is usually much less than the radius of the earth. As a result strong transverse dynamical forces are developed, which permit "dynamical" equilibrium of the bomber at heights far above the stationary ones.

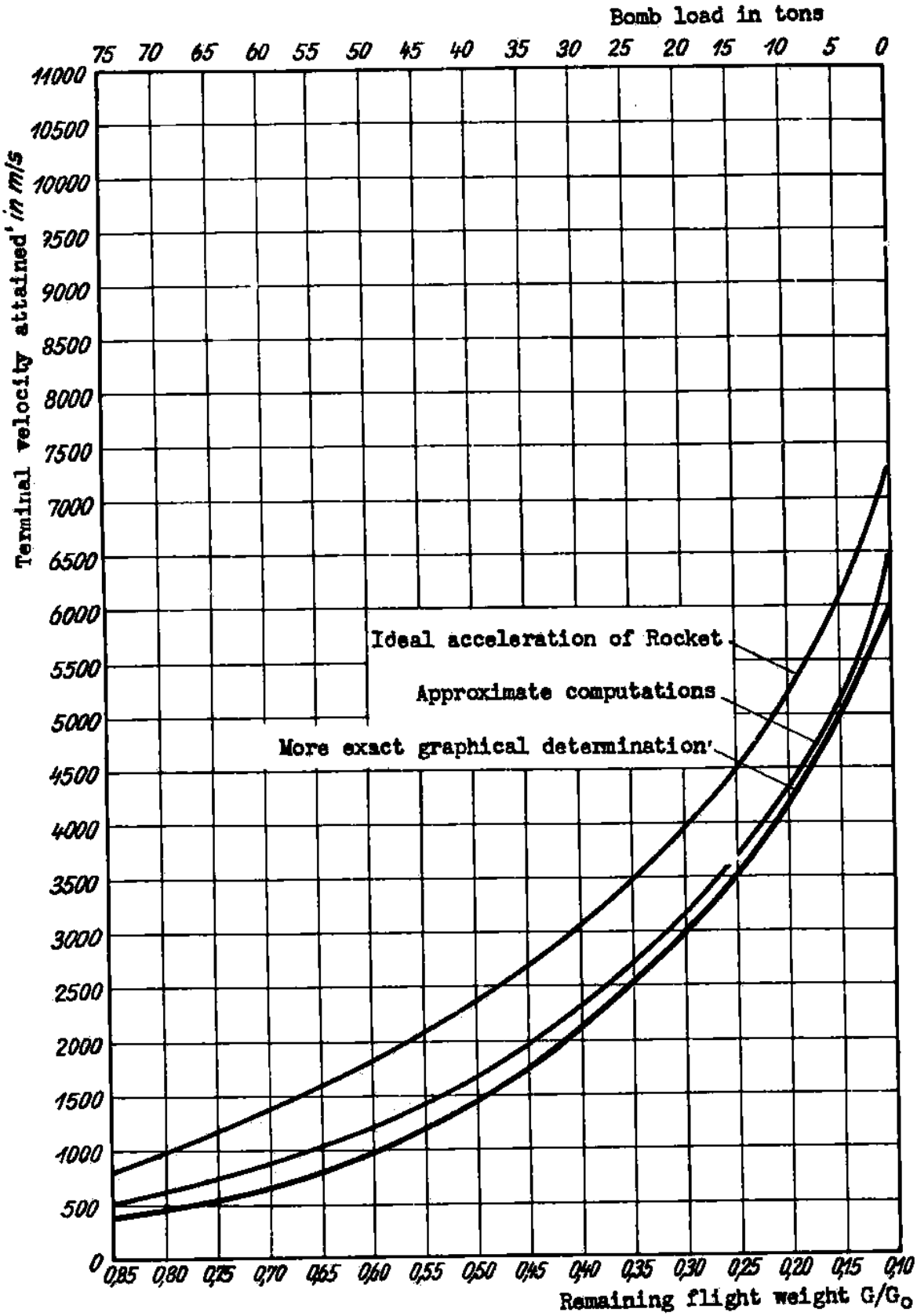

Fig. 65:

More exact determination of the relationship between bomb load, terminal velocity of the Rocket Bomber attained for v = 3000 m/sec and v_o = 284 m/sec by means of the graphical determination of the course. For comparison are plotted the approximate calculations and the curve for ideal Rocket acceleration.

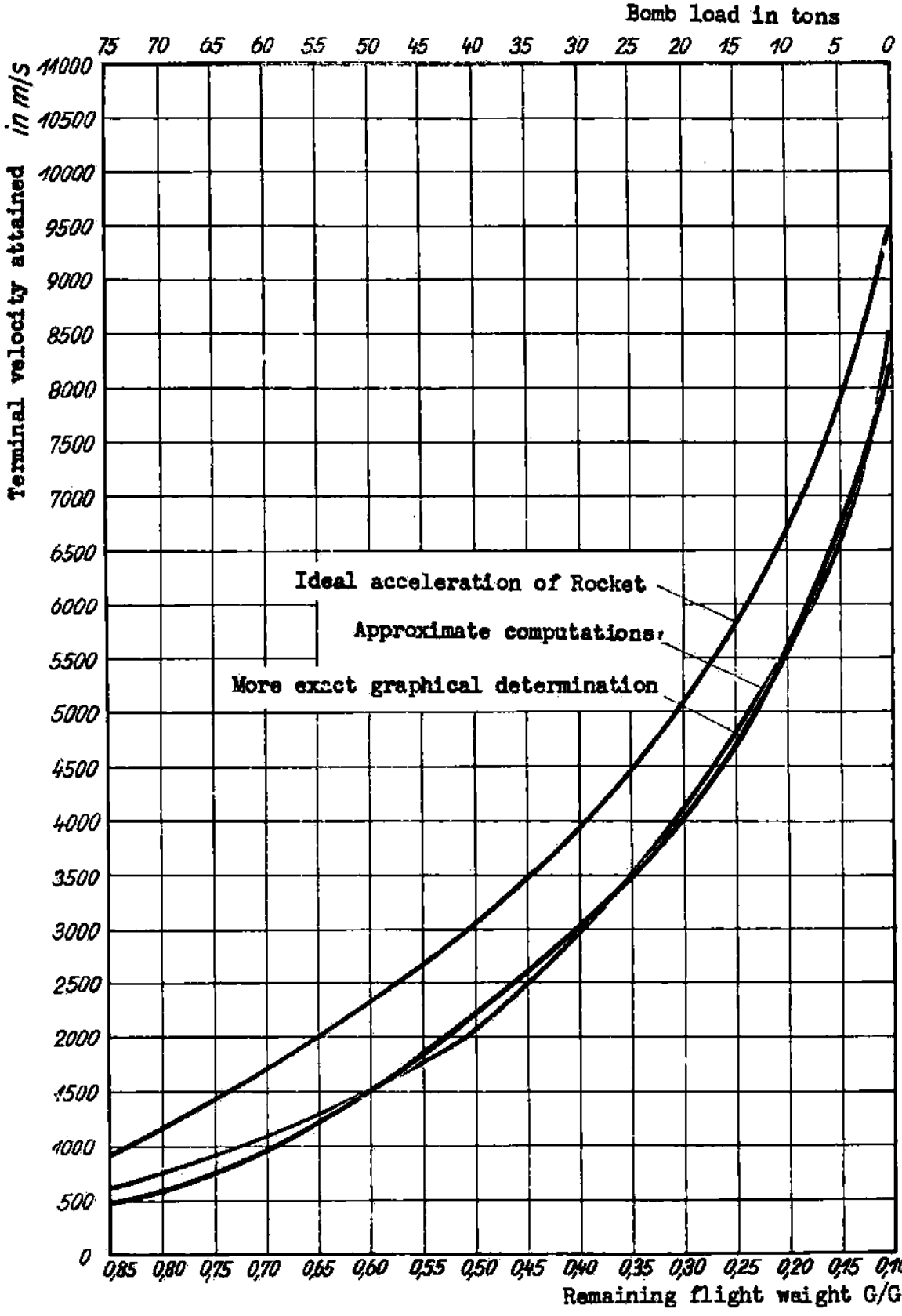

Fig. 66:

More exact determination of the relationship between bomb load, terminal velocity of the Rocket Bomber attained for $v = 4000$ m/sec and $v_o = 284$ m/sec by means of the graphical determination of the course. For comparison are plotted the approximate calculations and the curve for ideal Rocket acceleration.

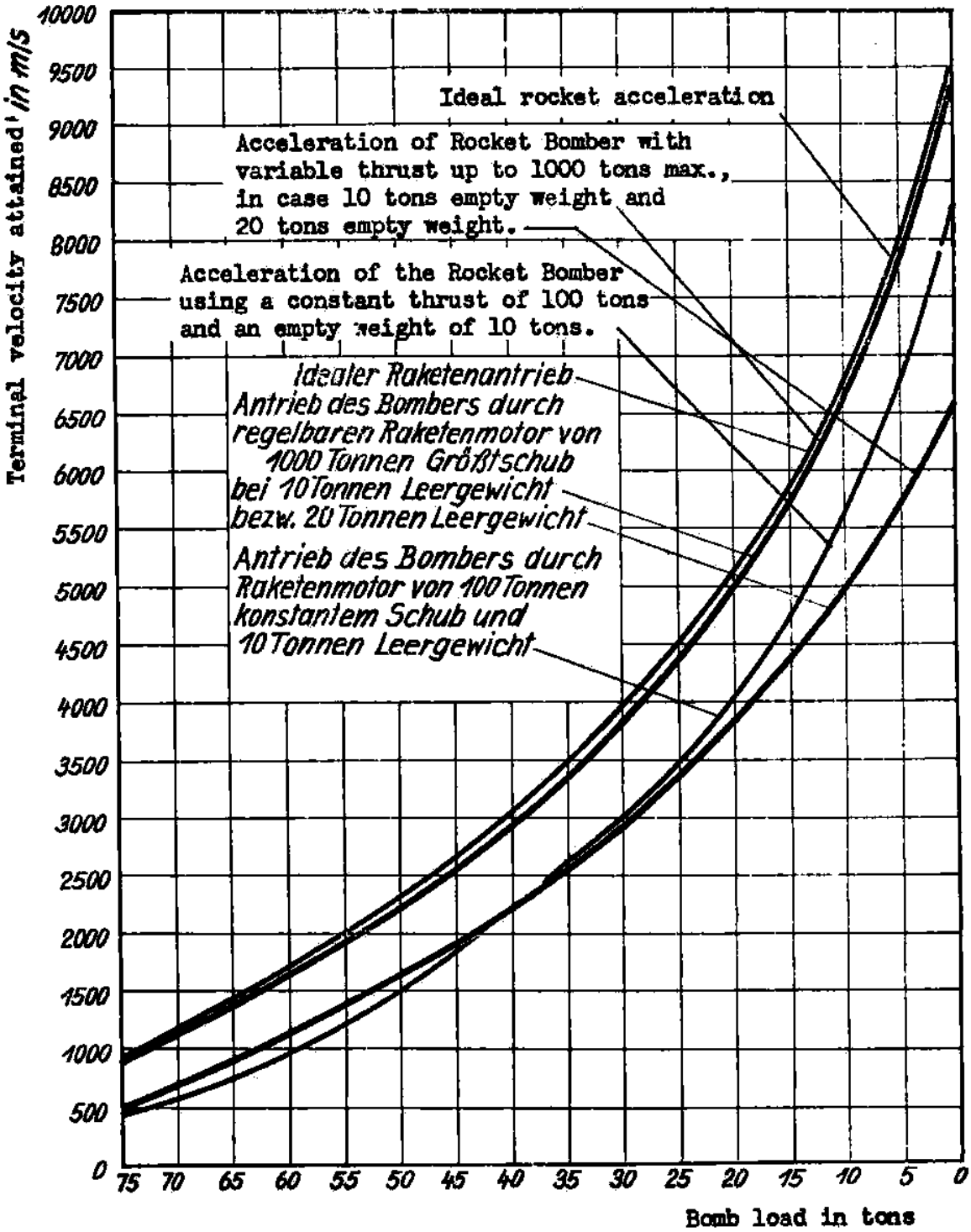

Fig. 67:

Climb of a Rocket Bomber whose thrust is adjustable between 100 and 1000 tons, i.e. high almost constant acceleration with c = 4000 m/sec exhaust velocity.

The actual heights oscillate about the stationary ones, with very large amplitude, while the additional dynamical forces tend to bring the aircraft back to the position of stationary equilibrium; i.e., they are restoring forces pointing toward the stationary position and increasing with distance of the aircraft from it, like spring-forces. The number of oscillations; for the example shown in Fig. 68, is not quite 2 for the whole climb; this is shown by the following consideration.

At first, the stationary altitude is greatly exceeded. This results from the fact that initially the air density decreases more slowly than the increase in velocity, so that the aircraft takes on a very steep position at angles $\varphi = 45^\circ$ or more. Already at fairly high velocities, the aircraft must now be turned through more than 45° from this position to that of horizontal flight. Because of the small radius of curvature available, this results in powerful centrifugal forces, which drive the aircraft up above the stationary equilibrium heights of 40-60 km, to heights over 100 km. One might now expect that the aircraft would immediately drop down again from these extreme altitudes, since the path is approaching parallelism with the earth's surface, and the radius of curvature is approaching the value of the earth's radius. This drop from the heights initially attained occurs only in slight degree, if at all, because in the meantime the velocity has increased very rapidly, and is already near the value V = 4700 m/sec for which the altitude of stationary equilibrium of the bomber becomes infinite. At this speed, the bomber is in stationary equilibrium at every altitude, so that it does not have to fall. If it exceeds V = 4700 m/sec, then it suddenly finds itself below the altitude of stationary equilibrium, so that it has an excess of buoyant force, and begins to climb again so long as the propulsion continues. This actual curve of climb is obtained from the exact calculation of the orbit, and is shown in Fig. 68. The whole climb may be considered as dynamic flight only in a limited sense. For the most part it follows an inertial path, like that of a projectile or a heavenly body, at heights which are practically in empty space, since one can no longer speak of an atmosphere in the sense of aerodynamics when the molecular free paths are greater than several hundred meters. Fig. 69, obtained from exact orbit calculations, shows the actual dynamical altitudes attained during the climb of the rocket bomber.

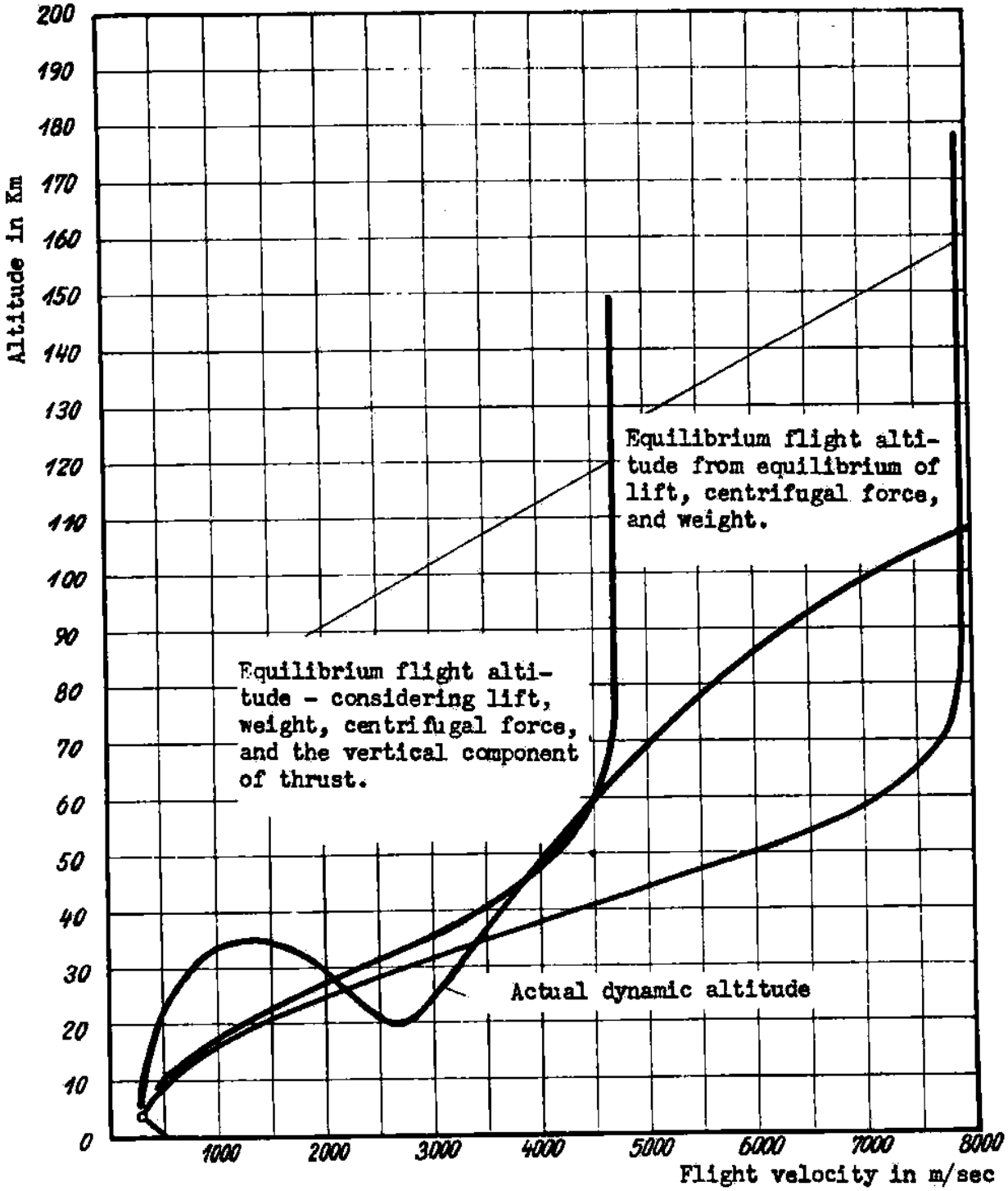

Fig. 68:

Comparison of stationary (i.e. instantaneous equilibrium) and actual, dynamic flight altitude when the Rocket Bomber is climbing with c = 4000 m/sec.

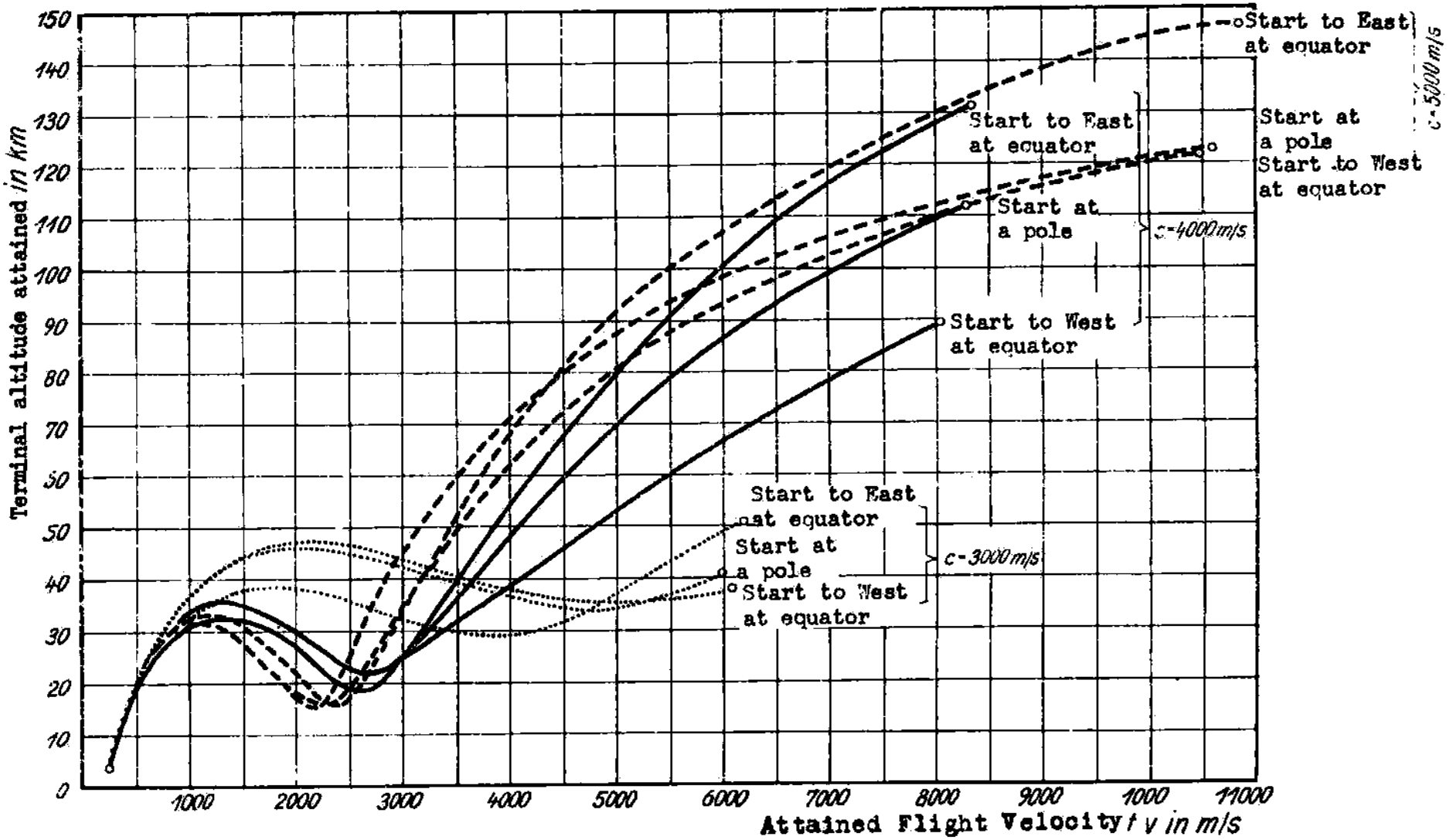

Fig. 69: Absolute climbing path of the Rocket Bomber with c = 3000, 4000 and 5000 m/sec, without consideration of the Earth's rotation, but with consideration of rotation velocity, of a point on Earth's equator, launch to East and launch to West.

IV. GLIDING FLIGHT AND LANDING

1. Supersonic Path of Gliding Flight

The supersonic path of gliding flight of the rocket bomber is determined by the forces acting on its center of mass, in the same manner as for the climb path. These external forces are: the weight of the aircraft, $G = mg_o \left(R/R + H\right)^2$, the aerodynamic lift $A = c_a F \rho v^2/2$, the air resistance $W = \varepsilon A$, and the d'Alembertian inertial force T. The same results apply to the rotation of the earth and the atmosphere as in Sec. III 3; in particular, the supersonic gliding path is to be considered as occurring in a plane, for an observer out in space; the deviating effect due to atmospheric rotation, which is especially effective in the lower layers of the atmosphere, must be eliminated by steering. Only in special cases will the Coriolis force be eliminated by steering, so that the orbit relative to the earth is plane; this will occur if the bomber is to go all around the earth on one hop, and land at its starting point. To do this in a perfectly plane absolute orbit is possible only if the takeoff field is at the pole, or if it is at the equator and the plane of the orbit coincides with the equatorial plane. Otherwise the procedure of circumnavigation will go as follows: until the bomb release an absolute plane orbit will be flown for purposes of precise celestial navigation; only the weather-vane action will be eliminated. After the bomb release a suitable relatively plane orbit will be flown, i.e., both weather-vane and Coriolis effects will be eliminated by steering. The arrangement of forces used in calculating the path are shown in Fig. 70 for gliding flight in two aspects, both viewed along the horizontal at the level of the aircraft. The procedure of calculation corresponds exactly to the stepwise method used in determining the climb path; first the absolute orbit is determined neglecting the Coriolis force and then the separately computed rotation of the earth is combined with the absolute orbit to give the desired relative orbit. The initial conditions for the decending path are given by the endpoint of the climb path. Since the climb path can be broken off at any point, there is a singly infinite manifold of possible paths of descent for each ascending path. Actually we started from the previously calculated ascending paths with c = 3, 4 and 5000 m/sec. and each of these was broken off at V_o = 1, 2, 3 up to 8000 m/sec, provided that all these velocities were actually reached. They represent the initial velocities for the descending path. Each descending path is followed until the velocity has dropped to 300 m/sec. In Figs. 71 and 72 two paths are shown; one for c = 3000 m/sec, V_o = 4000 m/sec; the other for c = 3000 m/sec, V_o=6000 m/sec at 6.36 times the altitude. In the figures, the strong oscillations of the paths, especially in the first portion, are notable. Because of the considerable tilt of the orbit resulting from the climb, the bomber overshoots its stationary altitude of flight, then approaches it from above, passes through it because of inertia, then is driven upward again by the greatly increased aerodynamic forces, until after several such oscillations the amplitude has decreased so much that the aircraft levels off at the stationary altitude and continues its flight at that altitude. This ricocheting generally has a favorable effect on the range of the bomber. It has the advantage that the thermal stresses of the external surfaces of the aircraft which face the course wind vary in time at high velocities of flight. The oscillation of the path will be hindered by steering, only if flight at the stationary altitude is needed for some special reason, say aiming before the bomb release.

Figs. 73 and 74 show the main elements of the two orbits in greater detail. In Fig. 74, one can easily see the following connections: the orbit shown in Fig. 72 is now represented by plotting the altitude H against the log of the distance S. One can easily locate the peaks and valleys of the orbit for both curves. The climb path ends after t = 300 sec. at an altitude H = 41.2 km, with inclination φ = 6.2°. At this moment the velocity V_o reaches 6000 m/sec. When the rocket motor is turned off the tangential acceleration drops from $b_t = +75.5\ m/sec^2$ to -5.5 m/sec^2, so the aircraft is greatly retarded, considering the flat ascending path. At the same time the normal acceleration acting at the cockpit drops from $b_n = +44\ m/sec^2$, after the normal component of the engine thrust has ceased, to $b_n = +18\ m/sec^2$. This positive residue results from the instantaneous center of curvature being above the aircraft. In the first part of its motorless supersonic glide path, the bomber climbs to H = 143.8 km, while the inclination of the path goes through a maximum $\varphi = +85°$ also the tangential acceleration gradually increases to $b_t = 0$ at the crest of the wave, while the normal acceleration increases up to $b_n = -10\ m/sec^2$, so that over a long period of time objects in the aircraft will appear to be weightless. At the same time the velocity drops to a minimum of V = 5800 m/sec at the crest of the wave. At the position, S = 1700 km, of the first crest in the orbit, the curves for φ and also practically for b_t (because of the low air-density) must go to zero, while b_n and V pass through a minimum. Then follows the first flight into a valley, with a height loss of 108.8 km. in 250 sec. During this the velocity again rises to 6000 m/sec, the largest inclination is -8°, the largest tangential acceleration is $b_t = +1\ m/sec^2$. In the trough the height is H = 35 km, and the largest normal acceleration acting at the cockpit is $b_n = +58\ m/sec^2$

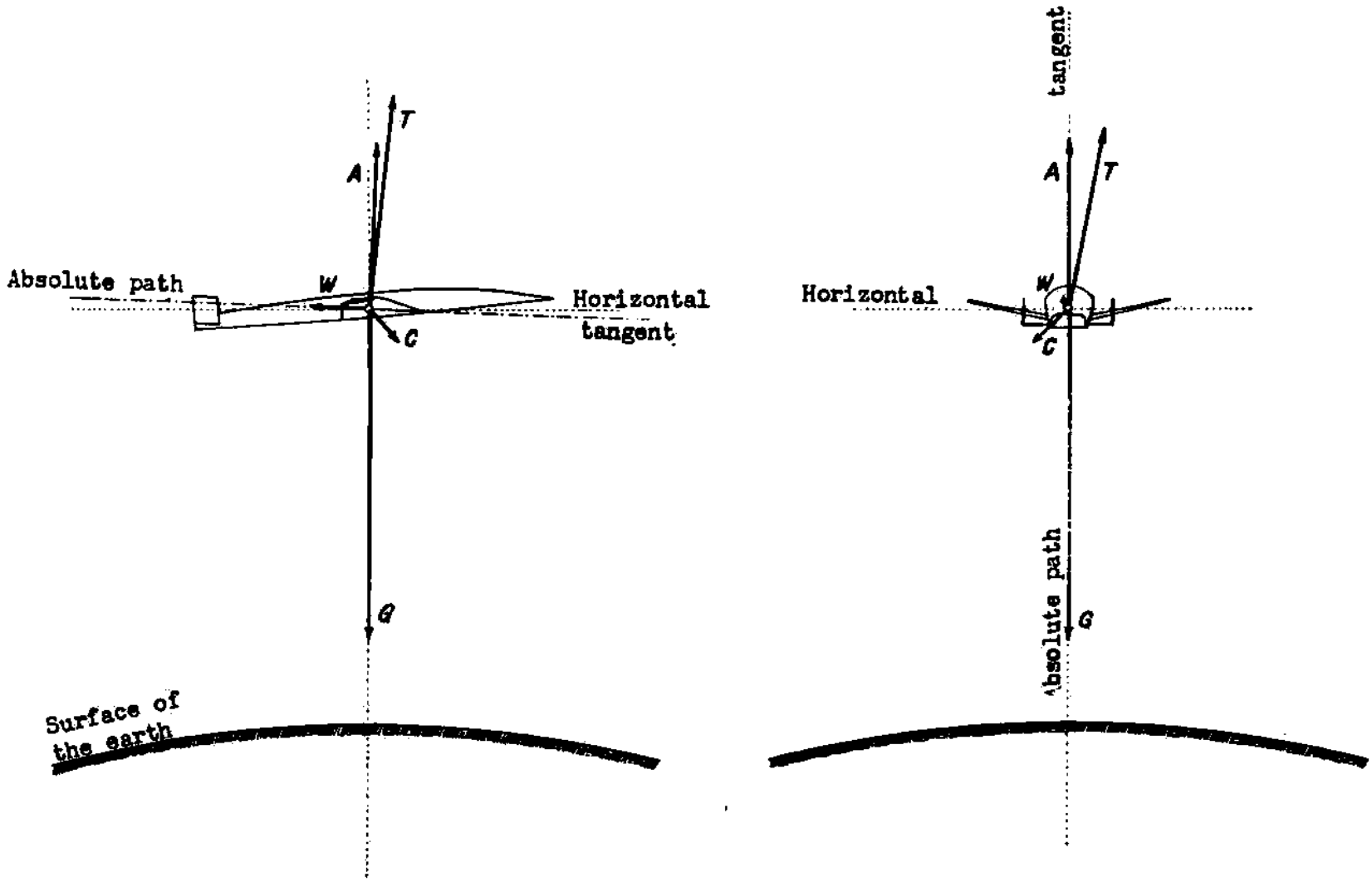

Fig. 70: External forces on the Rocket Bomber in the case of supersonic gliding.

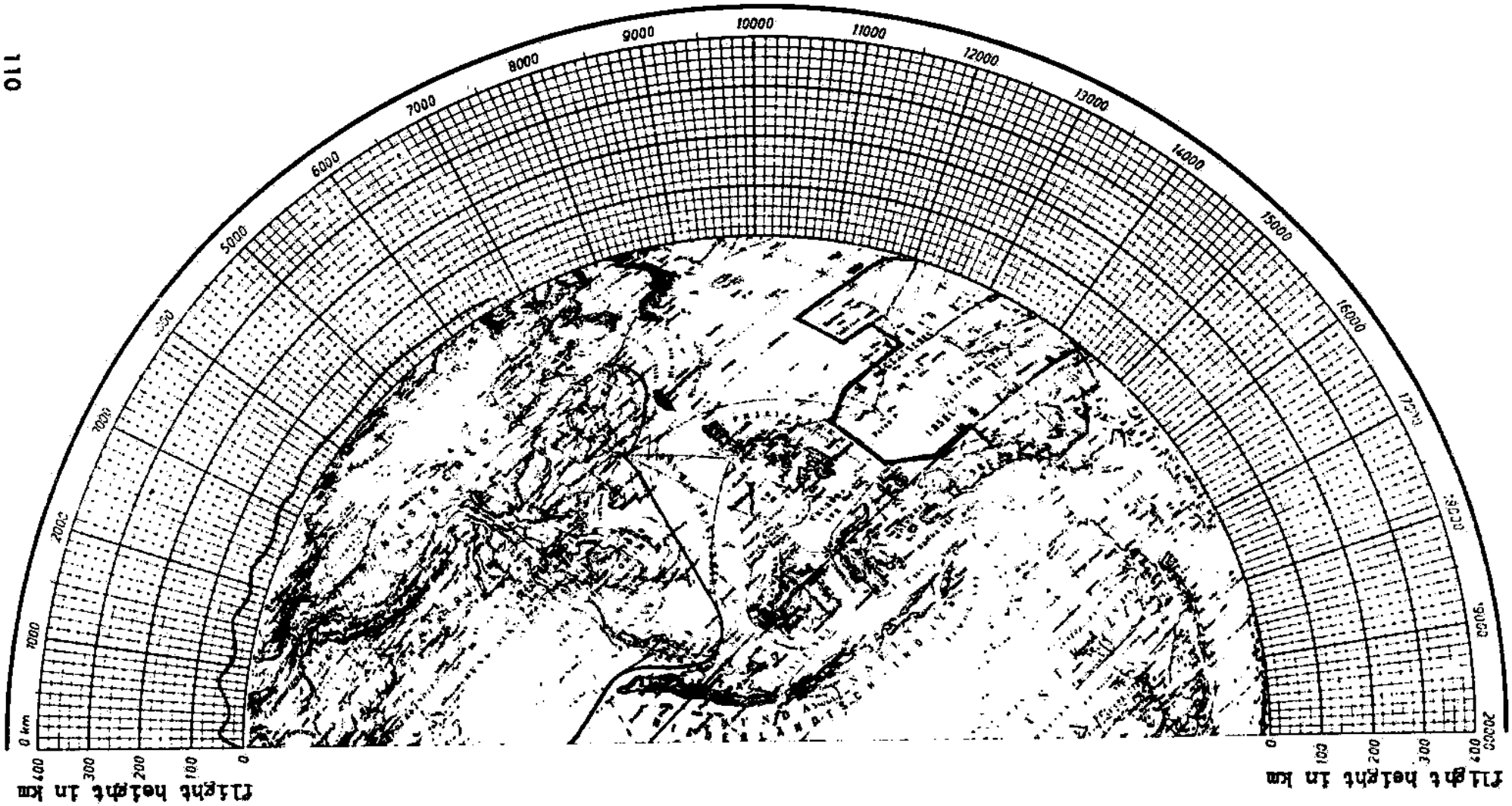

Fig. 71: Flight path of the Rocket Bomber with c = 3000 m/sec, v_o = 4000 m/sec and a bomb load of 11.5 tons.